

## Conventional and Neo-Antigenic Peptides Presented by $\beta$ Cells Are Targeted by Circulating Naïve CD8+ T Cells in Type 1 Diabetic and Healthy Donors

This is a pre print version of the following article:

*Original:*

Gonzalez-Duque, S., Azoury, M.E., Colli, M.L., Afonso, G., Turatsinze, J., Nigi, L., et al. (2018). Conventional and Neo-Antigenic Peptides Presented by  $\beta$  Cells Are Targeted by Circulating Naïve CD8+ T Cells in Type 1 Diabetic and Healthy Donors. CELL METABOLISM, 28(6), 946-960.e6 [10.1016/j.cmet.2018.07.007].

*Availability:*

This version is available <http://hdl.handle.net/11365/1058265> since 2018-09-04T11:49:21Z

*Published:*

DOI:10.1016/j.cmet.2018.07.007

*Terms of use:*

Open Access

The terms and conditions for the reuse of this version of the manuscript are specified in the publishing policy. Works made available under a Creative Commons license can be used according to the terms and conditions of said license.

For all terms of use and more information see the publisher's website.

(Article begins on next page)

# **Conventional and neo-antigenic peptides presented by $\beta$ cells are preferentially targeted in the pancreas, but not in blood, of type 1 diabetic patients**

Sergio Gonzalez-Duque<sup>1-4</sup>, Marie Eliane Azoury<sup>1-3</sup>, Maikel L. Colli<sup>5</sup>, Georgia Afonso<sup>1-3</sup>, Jean-Valery Turatsinze<sup>5</sup>, Laura Nigi<sup>6</sup>, Ana Ines Lalanne<sup>1-3</sup>, Guido Sebastiani<sup>6</sup>, Alexia Carré<sup>1-3</sup>, Sheena Pinto<sup>7</sup>, Slobodan Culina<sup>1-3</sup>, Noémie Corcos<sup>1-3</sup>, Marco Bugliani<sup>8</sup>, Piero Marchetti<sup>8</sup>, Mathieu Armanet<sup>9</sup>, Marc Diedisheim<sup>1-3,10</sup>, Bruno Kyewski<sup>7</sup>, Lars M. Steinmetz<sup>11,12</sup>, Søren Buus<sup>13</sup>, Sylvaine You<sup>1-3</sup>, Daniele Dubois-Laforgue<sup>1-3,10</sup>, Etienne Larger<sup>1-3,10</sup>, Jean-Paul Beressi<sup>14</sup>, Graziella Bruno<sup>15</sup>, Francesco Dotta<sup>6</sup>, Raphael Scharfmann<sup>1-3</sup>, Decio L. Eizirik<sup>5\*</sup>, Yann Verdier<sup>4\*</sup>, Joelle Vinh<sup>4\*</sup>, Roberto Mallone<sup>1-3,10\*\*</sup>.

<sup>1</sup>INSERM, U1016, Cochin Institute, Paris, F-75014, France.

<sup>2</sup>CNRS, UMR8104, Cochin Institute, Paris, F-75014, France.

<sup>3</sup>Paris Descartes University, Sorbonne Paris Cité, Paris, F-75014, France.

<sup>4</sup>ESPCI Paris, PSL University, Spectrométrie de Masse Biologique et Protéomique, CNRS USR3149, Paris, F-75005, France.

<sup>5</sup>Université Libre de Bruxelles Center for Diabetes Research and Welbio, Medical Faculty, Université Libre de Bruxelles, Brussels, B-1070, Belgium.

<sup>6</sup>University of Siena, Department of Medicine, Surgery and Neuroscience, Diabetes Unit and Fondazione Umberto di Mario ONLUS, Toscana Life Sciences, Siena, I-53100, Italy.

<sup>7</sup>DKFZ, Division of Developmental Immunology, Heidelberg, D-69120, Germany.

<sup>8</sup>University of Pisa, Department of Clinical and Experimental Medicine, Pisa, I-56124, Italy.

<sup>9</sup>Assistance Publique Hôpitaux de Paris, Cell Therapy Unit, Saint Louis Hospital, Paris, F-75010, France.

<sup>10</sup>Assistance Publique Hôpitaux de Paris, Service de Diabétologie, Cochin Hospital, Paris, F-75014, France.

<sup>11</sup>Stanford University, School of Medicine, Department of Genetics and Stanford Genome Technology Center, Stanford, 94305, USA.

<sup>12</sup>European Molecular Biology Laboratory, Genome Biology Unit, Heidelberg, D-69117 Germany.

<sup>13</sup>Panum Institute, Department of International Health, Immunology and Microbiology, Copenhagen, DK-2200, Denmark.

<sup>14</sup>Centre Hospitalier de Versailles André Mignot, Service de Diabétologie, Le Chesnay, F-78150, France.

<sup>15</sup>University of Turin, Department of Medical Sciences, Turin, I-10126, Italy.

\*These authors contributed equally to this work

\*\*Correspondence and Lead Contact: roberto.mallone@inserm.fr

## SUMMARY

Although CD8<sup>+</sup> T-cell-mediated autoimmune  $\beta$ -cell destruction occurs in type 1 diabetes (T1D), the target epitopes processed and presented by  $\beta$  cells are unknown. To identify them, we combined peptidomics and transcriptomics strategies. Inflammatory cytokines increased peptide presentation *in vitro*, paralleling upregulation of Human Leukocyte Antigen (HLA) Class I expression. Peptide sources featured several insulin granule proteins and all known  $\beta$ -cell antigens, barring islet-specific glucose-6-phosphatase catalytic subunit-related protein. Preproinsulin yielded HLA-A2-restricted epitopes previously described. Secretogranin V and its mRNA splice isoform SCG5-009, proconvertase-2, urocortin-3, the insulin gene enhancer protein ISL-1 and an islet amyloid polypeptide transpeptidation product emerged as antigens processed into HLA-A2-restricted epitopes which, as those already described, were recognized by circulating naïve CD8<sup>+</sup> T cells in T1D and healthy donors, and by pancreas-infiltrating cells in T1D donors. This peptidome opens new avenues to understand antigen processing by  $\beta$  cells and for developing T-cell biomarkers and tolerogenic vaccination strategies.

**Keywords:** antigen, autoimmunity,  $\beta$  cell, epitope, Human Leukocyte Antigen (HLA), preproinsulin, T cell, type 1 diabetes.

## INTRODUCTION

Autoimmune CD8<sup>+</sup> T cells dominate the pancreatic immune infiltrates of human type 1 diabetes (T1D) (Coppieters et al., 2012), and lyse  $\beta$  cells by recognizing surface peptide-Human Leukocyte Antigen Class I (pHLA-I) complexes. Identifying these peptides is therefore critical for developing tolerogenic vaccination strategies and immune staging tools targeting islet-reactive CD8<sup>+</sup> T cells.

Most islet antigens (Ags), namely insulin (INS) and its precursor preproinsulin (PPI), glutamic acid decarboxylase (GAD65/GAD2), islet Ag (IA)-2 (PTPRN) (Mallone et al., 2007; Martinuzzi et al., 2008), and zinc transporter 8 (ZnT8/SLC30A8) (Scotto et al., 2012), have been identified based on their targeting by auto-antibodies (aAbs). Other Ags such as islet-specific glucose-6-phosphatase catalytic subunit-related protein (IGRP) (Mallone et al., 2007), chromogranin A (CHGA) (Li et al., 2015) and islet amyloid polypeptide (IAPP) (Standifer et al., 2006) have been identified based on studies in the non-obese diabetic mouse and/or their islet-enriched expression. A systematic discovery effort is missing, and the available catalogue may be biased by the lack of information about the peptides that are naturally processed and presented by  $\beta$  cells.

Mutated sequences in tumor proteins become preferential CD8<sup>+</sup> T-cell targets (Gubin et al., 2014), possibly because they are regarded as non-self and therefore not efficiently tolerized. Similarly, other processes in  $\beta$  cells may facilitate tolerance escape: post-translational modifications (PTMs) (McGinty et al., 2014; Rondas et al., 2015), transpeptidation, i.e. the splicing and fusion of non-contiguous peptide fragments from the same protein or from different ones (Babon et al., 2016; Delong et al., 2016), and the use of alternative transcription start sites (Kracht et al., 2017). These studies have mostly focused on CD4<sup>+</sup> T cells, which are stimulated by pHLA Class II complexes presented by professional Ag-presenting cells that uptake  $\beta$ -cell material. These indirect Ag processing pathways do not reflect those that are

specific to  $\beta$  cells. Indeed, several arguments suggest an active role of  $\beta$  cells in their own demise (Eizirik et al., 2009).

First, we recently showed that some T1D susceptibility gene variants modulate islet inflammation (Marroqui et al., 2015; Marroqui et al., 2014; Moore et al., 2009), suggesting that the  $\beta$ -cell response to inflammation is genetically modulated. This response triggers cytokine/chemokine release, endoplasmic reticulum (ER) stress and HLA-I upregulation (Eizirik et al., 2009; Marroqui et al., 2017), which facilitate a productive autoimmune response. The alternative mRNA splicing signature induced by  $\beta$ -cell inflammation (Eizirik et al., 2012; Ortis et al., 2010) has received less attention, but may similarly generate neo-sequences not translated in the thymus and regarded as non-self.

Second, we recently reported a circulating islet-reactive CD8<sup>+</sup> T-cell repertoire that is predominantly naïve and largely overlapping between T1D and healthy subjects (Culina et al., 2018). These findings reveal a general leakiness of central tolerance irrespective of T1D status, begging the question of what determines T1D progression versus the maintenance of a ‘benign’ state of autoimmunity. One hypothesis is that the target  $\beta$  cell and its response to inflammation may be critical in the progression toward T1D in the face of similar autoimmune T-cell repertoires across individuals.

In this context, it is crucial to understand the ‘image’ that human  $\beta$  cells deliver to CD8<sup>+</sup> T cells through pHLA-I complexes. To this end, we implemented a strategy combining HLA-I peptidomics on  $\beta$  cells and RNAseq analysis of the splice isoforms transcribed by primary islets exposed or not to inflammatory cytokines and by thymic medullary epithelial cells (mTECs), focusing primarily on the most prevalent HLA-A2 variant.

## RESULTS

### **The HLA-I peptidome of human $\beta$ cells is enriched by cytokine exposure and displays the expected amino-acid length and motifs.**

Our first epitope discovery pipeline employed HLA-I peptidomics experiments on the ECN90  $\beta$ -cell line (Culina et al., 2018), which carries the HLA-I haplotype A\*02:01/A\*03:01/B\*40:01/B\*49:01/C\*03:04/C\*07:01 (A2/A3/B40/B49/C3/C7 from here on). ECN90  $\beta$  cells were cultured overnight with or without interferon (IFN)- $\gamma$ , alone or in combination with tumor necrosis factor (TNF)- $\alpha$  and interleukin (IL)-1 $\beta$ , and lysed to immunopurify pHLA-I complexes. HLA-I-bound peptides were then analyzed by liquid chromatography-tandem mass spectrometry (LC-MS/MS). Although ECN90  $\beta$  cells expressed surface HLA-I under basal conditions, this expression was significantly upregulated upon cytokine treatment (Fig. 1A-B), without significant cell death (Culina et al., 2018). The 2,997 eluted peptides were mostly (93%) 8-12-mers (Fig. 1C), i.e. the length required for HLA-I binding. The amino acid (aa) identity at pHLA-I anchor positions (p2 and p9) also revealed the preferences expected based on the aforementioned HLA-I haplotype (Fig. 1D-E). In line with the observed HLA-I upregulation, the number of eluted peptides was significantly higher in the presence of cytokines, and higher in  $\beta$  cells exposed to IFN- $\gamma$ , TNF- $\alpha$  and IL-1 $\beta$  compared with IFN- $\gamma$  alone (Fig. 1F).

These peptide datasets were subsequently analyzed using a stepwise bioinformatics pipeline (Fig. 1G). First, only peptides that were reproducibly detected in at least 2 of 5 biological replicates (85%; all percentages are given in relation to the number of peptides retained by the previous filter) and that displayed the expected 8-12-aa length (93%) were selected.  $\beta$ -cell-enriched peptides (both conventional and with PTMs, excluding those derived from peptide or mRNA splicing; red pipeline in Fig. 1G) were subsequently filtered based on non-ubiquitous (16%) and enriched  $\beta$ -cell expression (34%) of their source proteins. For other non-

conventional peptides (i.e. PTM or transcriptional variants), no expression filter was applied, as these species could be  $\beta$ -cell-specific in spite of a ubiquitous expression of the source protein or mRNA. PTM peptides (methionine, tryptophan, histidine and cysteine oxidation tryptophan conversion to kynurenine) derived from ubiquitous proteins accounted for 8% of the whole dataset (blue pipeline in Fig. 1G). Compounds potentially corresponding to peptide splice variants (0.5%; brown pipeline) were identified using an in-house script ([Fig. S1](#) and [Data S1](#)) based on reported peptide splicing preferences (Berkers et al., 2015) applied to known and putative Ags.

For peptides derived from mRNA splice variants (dotted and green pipeline in Fig. 1G), the peptidomics dataset was interrogated against RNAseq datasets from primary human islets exposed or not to cytokines and from human mTECs ([Data S2](#)). First, higher gene expression can favor peptide processing and presentation. Hence, mRNA splice variants were selected based on a median Reads Per Kilobase per Million mapped reads (RPKM)>5 in islets (27%), based on the median RPKM of known islet Ags (Eizirik et al., 2012). Second, mRNA isoforms poorly expressed in mTECs might favor T-cell escape from clonal deletion. Thus, mRNA variants with a RPKM<0.1 in mTECs or with a fold-decrease>100 vs. islets were selected (6%). Third, we selected mRNA isoforms with >10-fold higher expression in islets vs. other tissues. We then analyzed the predicted aa neo-sequences encoded by these mRNA variants, yielding 88/166 mRNA variants (53%) and 336 peptide neo-sequences that were used to interrogate the HLA-I peptidomics dataset, with 2 hits found. Finally, each dataset was filtered to retain only those peptides found enriched in HLA-I- vs. mock-purified samples, leading to the overall exclusion of 48% hits. We focused on predicted HLA-A2-restricted peptides for subsequent HLA-A2 binding and CD8<sup>+</sup> T-cell recognition studies. Collectively, these results show that inflammatory cytokines increase pHLA-I presentation and that these peptides display the aa signatures required for HLA-I binding.

**pHLA-I complexes from human  $\beta$  cells are enriched in peptides derived from secretory granule proteins, including known PPI epitopes.**

The filtered HLA-I peptidomics dataset obtained is described in [Fig. 2](#) and detailed in [Table S1](#). While 42/98 (43%) eluted peptides were shared among basal and cytokine-treated conditions, 45/98 (46%) peptides were only detected upon cytokine exposure ([Fig. 2A](#)). Also quantitatively, most peptides (62/98; 63%) were exclusively or more presented in cytokine-treated ECN90  $\beta$  cells (Table S1).

Among the 40 source proteins of HLA-I-eluted peptides ([Fig. 2B](#)), the most represented ones were the known islet Ags CHGA (n=15 peptides) and PPI (n=12, plus one derived from an INS-006 mRNA splice variants). Besides the other known Ag IA-2 (PTPRN; n=3), the 5 top scoring proteins included two putative Ags: Kinesin Family Member 1A (KIF1A; n=9) and Secretogranin V (SCG5/7B2; n=3, plus one derived from a SCG5-009 mRNA splice variant). Other proteins included known Ags, i.e. GAD2 (GAD65), SLC30A8 (ZnT8) and IAPP (splice peptide), and several putative ones. Notably, all the HLA-A2-restricted PPI peptides identified, namely PPI<sub>2-10</sub>, PPI<sub>6-14</sub>, PPI<sub>15-24</sub>, PPI<sub>29-38</sub> (INS<sub>B5-14</sub>) and PPI<sub>34-42</sub> (INS<sub>B10-18</sub>) ([Fig. 2C](#)), are already described as major CD8<sup>+</sup> T-cell epitopes, thus validating our discovery strategy. Source proteins were enriched for insulin granule products (14/42, 33%; [Fig. 2D](#)), namely CHGA, INS, SCG5, PTPRN, ATP-binding cassette sub-family C member 8 (ABCC8), proprotein convertase 1 (PCSK1/PC1), urocortin-3 (UCN3), chromogranin B (CHGB), carboxypeptidase E (CPE), proprotein convertase 2 (PCSK2/PC2), secretogranin III (SCG3), SLC30A8; and IAPP and neuropeptide Y (NPY) generating splice peptides. The predicted HLA-I restrictions of these peptides ([Fig. 2E](#)) comprised all the alleles expressed by ECN90  $\beta$  cells, while 10% of restrictions could not be assigned. For peptides derived from  $\beta$ -cell-enriched proteins, 11/98 (11%) carried PTMs, with most of them (8/11; 73%)



representing variants of unmodified peptides identified in this same dataset. Most of these modifications (7/11; 64%) were M(+15.99) methionine, C(+47.98) cysteine and W(+15.99) tryptophan oxidations, with W(+3.99) tryptophan to kynurenine transitions also detected. The 99 PTM peptides derived from ubiquitous source proteins are listed in [Table S2](#).

To validate the results obtained using the ECN90  $\beta$ -cell line, a HLA-A2<sup>+</sup> primary human islet preparation that did not share other HLA-I alleles with ECN90 cells was analyzed similarly. The major source proteins of the HLA-I-bound peptides identified were largely overlapping with those found in ECN90 cells ([Fig. 2F](#)), with INS (n=12 peptides), CHGA (n=4), KIF1A (n=3) and SCG5 (n=3) ranking highest for both cells, and CHGB (n=3), PCSK2 (n=1) and an identical IAPP splice peptide also detected in both. When analyzing the identity of individual peptides (including length and PTM variants) ([Table S3](#)), 16/33 (48%) were shared between ECN90 and primary islet cells. This common repertoire increased to 12/13 peptides (92%) when considering only predicted HLA-A2 binders, supporting the validity of the ECN90  $\beta$ -cell model. Of note, shared peptides included all the PPI species already described as CD8<sup>+</sup> T-cell epitopes, SCG5<sub>186-196</sub> along with a shorter SCG5<sub>186-195</sub> variant with higher HLA-A2 affinity, and the IAPP<sub>15-17</sub>/IAPP<sub>5-10</sub> splice peptide VAL/KLQVFL. Although this product could also reflect PTPRN<sub>596-598</sub>/IAPP<sub>5-10</sub> *trans*-splicing, IAPP<sub>15-17</sub>/IAPP<sub>5-10</sub> is more likely because the intra-protein vicinity of these fragments is more favorable for transpeptidation. The new hits identified were mostly predicted to bind to the HLA-I molecules not shared with ECN90 cells, barring an HLA-A2-restricted CHGB<sub>440-448</sub> peptide retained for further validation. Contrary to ECN90 cells, most peptides were detected at similar levels under basal and cytokine-treated conditions ([Table S3](#)). This mirrored a higher basal HLA-I expression in primary islets, possibly reflecting peri-mortem and tissue isolation stress conditions, which was less upregulated by cytokine treatment ([Fig. 1G](#)). Moreover, detection sensitivity may have been limited by the concomitant isolation of non- $\beta$ -cell peptides, i.e. pancreatic

polypeptide- and glucagon-derived sequences likely eluted from  $\delta$  and  $\alpha$  cells (n=4 and 5, respectively; not shown because excluded by the  $\beta$ -cell enrichment filter).

The fragmentation profile of the identified peptides was confirmed by comparing their MS/MS spectra with those of the corresponding synthetic peptides. Finally, the predicted HLA-A2 binding was experimentally verified (Fig. S2A-H), leading to the final selection of 18/19 (95%) HLA-I-eluted peptides for CD8<sup>+</sup> T-cell studies (including CHGB<sub>440-448</sub> eluted from primary islets).

Collectively, these data show that  $\beta$  cells process and present several known HLA-A2-restricted PPI epitopes and additional candidate ones, which are enriched for secretory granule products.

***In silico* analysis of mRNA splice variants yields additional predicted neo-Ag peptides.**

The RNAseq dataset used for assigning *m/z* species was further mined *in silico*, independently of the HLA-I peptidomics pipeline, to identify other potential HLA-A2-restricted peptides (Fig. 1G, dotted pipeline). Selection was based on a predicted HLA-A2 binding, a 9-10-aa length and a neo-sequence stretch  $\geq 3$  aa, with 39 candidates retained (Fig. S2I). These were splice variants of known  $\beta$ -cell Ags (GAD2-003, IAPP-002, IAPP-004, PTPRN-021, SLC30A8-002) and of candidate ones. Most of the source mRNA splice variants (35/39, 90%) were similarly expressed in untreated and cytokine-treated islets. HLA-A2 binding was experimentally confirmed for 34/39 candidates (87%; Fig. S2I), which were retained for further validation along with the 18 HLA-A2 binders identified by HLA-I peptidomics.

**HLA-A2-restricted  $\beta$ -cell peptides are targeted by a circulating naïve CD8<sup>+</sup> T-cell repertoire in healthy donors.**

We previously documented that the vast majority of individuals, both type 1 diabetic and healthy, harbor similar frequencies of circulating, predominantly naïve HLA-A2-restricted CD8<sup>+</sup> T cells reactive to known PPI, GAD65, IA-2, IGRP and ZnT8 epitopes (Culina et al., 2018). Similarly, we reasoned that the presence of a cognate naïve CD8<sup>+</sup> T-cell repertoire is the preliminary requirement for the immunogenicity of the HLA-A2-restricted candidate epitopes identified in the *in vitro* HLA-I peptidomics and *in silico* transcriptomics pipeline (n=52; 18 and 34, respectively). We therefore started by screening these candidates for recognition by circulating CD8<sup>+</sup> T cells in HLA-A2<sup>+</sup> healthy donors ([Table S4](#)), using combinatorial double-coded HLA-A2 multimers (MMrs) loaded with the corresponding synthetic peptides (Culina et al., 2018). We retained those candidates that harbored a cognate naïve CD8<sup>+</sup> T-cell repertoire, based on *i*) the frequency of this repertoire, which is typically in the range of 1-50/10<sup>6</sup> CD8<sup>+</sup> T cells (Alanio et al., 2010; Culina et al., 2018); and *ii*) the pattern of HLA-A2 MMr staining, which is usually clustered rather than spread in the presence of a specific epitope-reactive population (James et al., 2018). The gating strategy is presented in [Fig. 3](#) and representative dot plots in [Fig. 4A-F](#). Using these two criteria, several candidate epitopes displayed a cognate naïve CD8<sup>+</sup> T-cell repertoire in the expected range in a sizable fraction ( $\geq 50\%$ ) of the healthy individuals analyzed. The frequency of CD8<sup>+</sup> T cells recognizing the known  $\beta$ -cell epitope PPI<sub>6-14</sub> previously analyzed (Culina et al., 2018) also fell in the same range, with some outliers noted. In total, 9/18 HLA-I-eluted peptides (50%; [Fig. 4G](#)) were validated, namely CHGA<sub>344-352</sub>, insulin gene enhancer protein ISL<sub>1276-284</sub>, potassium channel subfamily K member 16 (KCNK16)<sub>129-137</sub>, KIF1A<sub>1347-1355</sub>, PCSK2<sub>30-38</sub>, SCG5<sub>186-195</sub>, SCG5-009<sub>186-194</sub> and UCN3<sub>1-9</sub>. Despite recognition in only 1 of 6 donors analyzed, the peptide splice product IAPP<sub>15-17</sub>/IAPP<sub>5-10</sub> was also retained, since it was identified in both ECN90 and primary islet cells. Using the same criteria, 11/34 candidates selected *in silico* were validated (32%; [Fig. 4H](#)), namely cyclin I (CCNI)-008<sub>14-22</sub>, GAD2-

003<sub>179-187</sub>, guanine nucleotide-binding protein G(s) subunit  $\alpha$  isoforms short (GNAS)-036<sub>67-75</sub>, GNAS-036<sub>124-132</sub>, IAPP-002<sub>33-42</sub>, PTPRN-021<sub>392-402</sub>, PTPRN-021<sub>398-407</sub>, phogrin/receptor-type tyrosine-protein phosphatase N2 (PTPRN2)-005<sub>11-19</sub>, PTPRN2-005<sub>19-27</sub>, mitochondrial oligoribonuclease (REXO2)-020<sub>2-10</sub>, and SLC30A8-002<sub>16-25</sub>. As previously observed for other known  $\beta$ -cell epitopes (Culina et al., 2018), including the PPI<sub>6-14</sub> here used as  $\beta$ -cell positive control, only a minority (median 16.4%, interquartile range 8.5-26.7%) of CD8<sup>+</sup> T cells recognizing these candidate epitopes were Ag-experienced (CD45RA<sup>+</sup>CCR7<sup>-</sup>, CD45RA<sup>-</sup>CCR7<sup>-</sup> or CD45RA<sup>-</sup>CCR7<sup>+</sup>; Fig. 4I-J). Conversely, the Flu MP<sub>58-66</sub> peptide included as viral positive control displayed the expected predominantly Ag-experienced phenotype. The complete list of the 20 candidates validated for CD8<sup>+</sup> T-cell recognition is presented in Table 1. All the peptides validated came from source proteins whose gene expression was detected in islets, both under basal and cytokine-treated conditions. One notable exception was SCG5-009, whose expression was negligible under basal condition but strongly upregulated after cytokine treatment. Gene expression in mTECs was also negligible in all cases, with the exception of CHGA, ISL1 and SCG5.

Collectively, these results show that most of the  $\beta$ -cell peptides identified display a cognate naïve CD8<sup>+</sup> T-cell repertoire in the blood of healthy individuals, making them potential targets of islet autoimmunity.

**Circulating CD8<sup>+</sup> T cells reactive to HLA-A2-restricted  $\beta$ -cell peptides display similar *ex-vivo* frequencies and a predominantly naïve phenotype in T1D and healthy subjects.**

Thirteen of the 20  $\beta$ -cell peptides validated for recognition by a naïve CD8<sup>+</sup> T-cell repertoire were selected for further *ex-vivo* combinatorial double-coded MMr validation using blood samples from HLA-A2<sup>+</sup> recent-onset T1D and healthy subjects (n=10/each; Table S4). For naturally processed and presented peptides identified by HLA-I peptidomics, we focused on 6

insulin granule putative Ags, namely IAPP<sub>15-17/5-10</sub>, PCSK2<sub>30-38</sub>, SCG5<sub>186-195</sub>, SCG5-009<sub>186-194</sub> and UCN3<sub>1-9</sub>; and the transcription factor ISL1<sub>276-284</sub>. A less focused selection was made for 7 predicted mRNA splice peptides, as these may be derived from short-lived, unstable defective ribosomal products (DRiPs) (Anton and Yewdell, 2014). CCNI-008<sub>14-22</sub>, GAD2-003<sub>179-187</sub>, GNAS-036<sub>67-75</sub>, GNAS-036<sub>124-132</sub>, IAPP-002<sub>33-42</sub>, PTPRN2-005<sub>11-19</sub> and SLC30A8-002<sub>16-25</sub> were thus selected. The frequency of circulating CD8<sup>+</sup> T cells recognizing these peptides and the control PPI<sub>6-14</sub> epitope was similar in T1D and healthy subjects (Fig. 5A), and fell in the same range (1-50/10<sup>6</sup> CD8<sup>+</sup> T cells) detected in the preliminary screening performed on healthy subjects using different fluorochrome-labeled MMr combinations (Fig. 4G-H), with the exception of IAPP-002<sub>33-42</sub> for which virtually no MMr<sup>+</sup> cells were detected. As in the screening round, frequencies were particularly high and clustered for 4 CD8<sup>+</sup> T-cell specificities, namely SCG5-009<sub>186-194</sub>, UCN3<sub>1-9</sub>, CCNI-008<sub>14-22</sub> and GAD2-003<sub>179-187</sub>. As reported for PPI<sub>6-14</sub> and other known  $\beta$ -cell epitopes (Culina et al., 2018), these MMr<sup>+</sup> cells were predominantly naïve in both T1D and healthy subjects (Fig. 5B; median 8.3%, interquartile range 0-20.0%).

Collectively, these results show that the  $\beta$ -cell peptides identified are targeted by similar frequencies of predominantly naïve circulating CD8<sup>+</sup> T cells in T1D and healthy subjects.

### **Pancreas-infiltrating cells reactive to the HLA-A2-restricted IAPP<sub>15-17/5-10</sub>, ISL1<sub>276-284</sub> and UCN3<sub>1-9</sub> peptides are enriched in T1D patients.**

Given the lack of difference in frequency or markers of prior Ag encounter observed for circulating islet-reactive CD8<sup>+</sup> T cells between T1D and healthy donors, we verified whether these reactivities were present in the pancreas-infiltrating cells of HLA-A2<sup>+</sup> T1D, aAb<sup>+</sup>, non-diabetic and type 2 diabetes donors by *in-situ* MMr staining of consecutive tissue sections from the Network for Pancreatic Organ Donors (nPOD) repository. We selected IAPP<sub>15-17/5-10</sub>,

ISL1<sub>276-284</sub> and UCN3<sub>1-9</sub>, which are representative of the frequency range detected in peripheral blood and stained positive in a preliminary screening on pancreatic sections from one T1D donor (Fig. S3; with SCG-009<sub>186-194</sub> also staining positive). Fig. 6A-R displays representative images, with scattered MMr<sup>+</sup> cells in the vicinity of the islet or exocrine tissue. The  $\beta$ -cell ZnT8<sub>186-194</sub> peptide and the melanocyte MelanA<sub>26-35</sub> peptide provided positive and negative controls, respectively (Culina et al., 2018). Results are summarized in Fig. 6S and Table S5. Whereas IAPP<sub>15-17/5-10</sub>, ISL1<sub>276-284</sub>, UCN3<sub>1-9</sub> (and ZnT8<sub>186-194</sub>) MMr<sup>+</sup> cells were significantly more abundant than MelanA<sub>26-35</sub> MMr<sup>+</sup> cells in T1D, aAb<sup>+</sup> (barring UCN3<sub>1-9</sub>), and non-diabetic cases (barring IAPP<sub>15-17/5-10</sub> and UCN3<sub>1-9</sub>), all islet MMr<sup>+</sup> cells were enriched in the pancreata of T1D vs. non-diabetic cases, and also in the pancreata of aAb<sup>+</sup> vs. non-diabetic cases for IAPP<sub>15-17/5-10</sub> and ISL1<sub>276-284</sub>. In contrast, islet and MelanA<sub>26-35</sub> MMr<sup>+</sup> cells were present at similar densities across all groups in pancreatic lymph node (PLN) sections from the same donors (Fig. 6T), as reported for ZnT8<sub>186-194</sub> (Culina et al., 2018).

Fluorescent confocal microscopy on pancreas sections from one T1D donor (Fig. 6U-W) detected 60 CD8<sup>+</sup> cells (2.3 cells/mm<sup>2</sup>), among which 37 (61.7%) were CD45RO<sup>+</sup> and 2 CD45RO<sup>+</sup>MMr<sup>+</sup> using pooled IAPP<sub>15-17/5-10</sub>/ISL1<sub>276-284</sub>/UCN3<sub>1-9</sub> MMrs (5.4% of CD8<sup>+</sup>CD45RO<sup>+</sup> and 3.3% of total CD8<sup>+</sup> cells), suggesting that pancreas-infiltrating islet MMr<sup>+</sup> cells are Ag-experienced CD8<sup>+</sup> T cells.

Collectively, these results show that IAPP<sub>15-17/5-10</sub>-, ISL1<sub>276-284</sub>- and UCN3<sub>1-9</sub>-reactive cells are enriched in the pancreas of T1D patients, similarly to ZnT8<sub>186-194</sub>-reactive cells (Culina et al., 2018), lending support to their relevance in T1D.

## DISCUSSION

We here provide a first catalogue of the HLA-I peptidome of human  $\beta$  cells, using an immortalized  $\beta$ -cell line naturally expressing the most prevalent HLA-A2 variant. This cellular model proved informative, since several HLA-A2-restricted peptides identified were also naturally processed and presented by primary human islets. The technical strengths of our approach are the combined HLA-I peptidomics and transcriptomics pipelines; the use of small cell numbers ( $20 \times 10^6$ ) for HLA-I purification, despite its low expression in  $\beta$  cells compared with professional Ag-presenting cells; and the use of a mock immunopurification to exclude peptides not bound to HLA-I. One limitation is the lower sensitivity of the LC-MS/MS data-dependent acquisition discovery mode used compared with targeted strategies. Indeed, previous studies on mouse NIT-1  $\beta$  cells (Dudek et al., 2012) detected low amounts of the immunodominant IGRP<sub>206-214</sub> peptide only after using a targeted approach on IFN- $\gamma$ -treated cells. Nonetheless, our sensitivity proved sufficient to detect several known  $\beta$ -cell Ags. Although this did not allow a precise quantitation of pHLA-I complexes, it allowed to detect HLA-I-bound peptides without *a priori* hypotheses.

Expectedly, only ~5% of the HLA-I peptidome originated from proteins preferentially expressed in  $\beta$  cells. Multiple PPI peptides described as major CD8<sup>+</sup> T-cell epitopes were detected, validating our discovery approach and documenting their natural processing and presentation by  $\beta$  cells. Peptides derived from all the other known  $\beta$ -cell Ags were also identified, namely CHGA, PTPRN, GAD2, SLC30A8 and IAPP. The only known Ag missing was IGRP, which may reflect low amounts of IGRP pHLA-I complexes, as reported for murine NIT-1  $\beta$  cells (Dudek et al., 2012). The same may be true for the ZnT8<sub>186-194</sub> epitope, for which a concordant *m/z* value was identified at the MS1 level in several HLA-I-purified ECN90 samples (1/5, 5/5 and 4/5 for basal, IFN- $\gamma$ -treated and IFN- $\gamma$ /TNF- $\alpha$ /IL-1 $\beta$ -treated conditions, respectively; 1/15 mock-purified samples). More importantly, several as yet

undescribed peptides were identified, many of which were derived from secretory granule proteins, namely CHGA, INS, SCG5, PTPRN, ABCC8, PCSK1, UCN3, CHGB, CPE, PCSK2, SCG3, SCL30A8, NPY and IAPP. This is not surprising considering that granule proteins are abundantly synthesized by  $\beta$  cells, thus favoring HLA-I presentation (Bassani-Sternberg et al., 2015). Their fast turnover also increases the odds of producing misfolded proteins, which are rapidly routed toward proteasomal degradation and HLA-I presentation (Anton and Yewdell, 2014).

mRNA alternative splicing is another mechanism frequently leading to unstable DRiPs, which are rapidly degraded through different pathways (Anton and Yewdell, 2014). Moreover, these mRNA isoforms may translate aa neo-sequences when exons are either added or skipped compared to the canonical mRNA. We therefore performed a parallel *in silico* prediction of mRNA-translated peptide neo-sequences. Although no proof of natural processing and presentation could be provided for most of these theoretical peptide products, the finding of a naïve CD8<sup>+</sup> T-cell repertoire capable of recognizing them supports their potential relevance as autoimmune T-cell targets. Of note, peptides derived from the alternative open reading frame INS mRNA (Kracht et al., 2017) were not detected.

Despite presentation by HLA-I molecules, peptides may still be ignored by CD8<sup>+</sup> T cells, thus not triggering an autoimmune response. This primarily reflects the absence of a cognate naïve repertoire available for priming (Alanio et al., 2010). We therefore first screened healthy individuals for the presence of cognate naïve CD8<sup>+</sup> T cells, which were found for several peptides. Although the poor expression of the genes encoding these proteins in mTECs may exert a facilitating effect, this is not an absolute requirement for peripheral CD8<sup>+</sup> T-cell recognition. Indeed, *CHGA*, *ISL1* and *SCG5* were expressed in mTECs, and yet targeted by CD8<sup>+</sup> T cells at frequencies comparable to those of T cells recognizing Ags not expressed in



mTECs, in line with the increasing appreciation that thymic clonal deletion is highly incomplete (Culina et al., 2018).

Based on our previous findings on known  $\beta$ -cell epitopes (Culina et al., 2018), we did not expect differences in circulating CD8<sup>+</sup> T cells between T1D and healthy subjects, because the Ag-experienced fraction is rather limited, likely reflecting sequestration in the target tissue. This was also the case for the candidates studied herein, and for the well-described control PPI<sub>6-14</sub> epitope eluted from pHLA-I complexes. Together with the reactivity against IAPP<sub>15-17/5-10</sub>, ISL1<sub>276-284</sub> and UCN3<sub>1-9</sub>, which was preferentially detected in the pancreatic infiltrates of T1D (and aAb<sup>+</sup>) donors and localized in CD8<sup>+</sup>CD45RO<sup>+</sup> T cells in one T1D case, these findings provide a first validation of their disease relevance. The degree of evidence for a relevance to T1D is higher for those peptides targeted by CD8<sup>+</sup> T cells and naturally processed and presented by  $\beta$  cells, i.e. SCG5<sub>186-195</sub>, PCSK2<sub>30-38</sub>, UCN3<sub>1-9</sub> and ISL1<sub>276-284</sub>. These also include the neo-antigenic peptides SCG-009<sub>186-194</sub> and IAPP<sub>15-17/5-10</sub> generated by mRNA splicing and transpeptidation, respectively.

Complementary analyses of the current HLA-I peptidomics dataset will yield additional information. First, only few PTMs were searched and a dedicated analysis is required. This should include the distinction between biological and experimentally induced PTMs, since some of them, e.g. the tryptophan to kynurenine conversion of the PPI<sub>15-24</sub> peptide, were similarly detected in the corresponding synthetic peptides. Second, an unbiased analysis of transpeptidation beyond the described aa preference rules (Berkers et al., 2015) will likely yield additional fusion peptides, which may account for up to one third of the HLA-I peptidome (Liepe et al., 2016). Third, only HLA-A2-restricted peptides were analyzed for T-cell recognition, leaving several HLA-A3- and HLA-B39-restricted candidates available for follow-up studies. HLA-B39 was expressed by the primary islets analyzed and, although rare, is the HLA-I variant most strongly associated with T1D (Nejentsev et al., 2007).

Finally, the HLA-I peptidome obtained allows to formulate hypotheses about the Ag-processing pathways employed by  $\beta$  cells. Some peptides (UCN3<sub>1-9</sub>, IAPP<sub>15-17/5-10</sub>, PPI<sub>2-10</sub>, PPI<sub>6-14</sub>, PPI<sub>15-24</sub>) are located in the leader sequence of proteins abundantly produced by  $\beta$  cells, which is cleaved in the ER at each protein synthesis. These byproducts may therefore provide a rich peptide source for HLA-I presentation and likely follow alternative Ag-processing pathways within the ER, independent of proteasome cleavage (El Hage et al., 2008; Skowera et al., 2008). It is also noteworthy that several source proteins of HLA-I-bound peptides, i.e. CHGA, INS, SCG5, PCSK1, UCN3, CHGB, CPE, PCSK2, SCG3, NPY and IAPP are synthesized as precursors and incorporated into  $\beta$ -cell granules, where they undergo intermediate processing by proconvertases to yield bioactive products. A notable example is SCG5, a PCSK2 chaperone that is gradually degraded along the secretory pathway to competitively prevent the premature activation of PCSK2 by autocatalytic cleavage (Mbikay et al., 2001). This continuous degradation may explain the abundance of HLA-I-bound SCG5 peptides. In this respect, the C-terminal SCG5<sub>186-195</sub> peptide is located between furin (RRKRR) and PCSK2 (KK) cleavage sites and, similar to leader sequence peptides, may behave as a byproduct of the intermediate SCG5 processing (Bartolomucci et al., 2011). The same is true for several CHGA peptides, e.g. CHGA<sub>344-352</sub>, which maps to the WE-14 neuropeptide produced by CHGA cleavage at dibasic KR motifs (Bartolomucci et al., 2011). These peptides may access the HLA-I pathway following crinophagy, i.e. the disposal of unused secretory granules through fusion with lysosomes (Goginashvili et al., 2015; Weckman et al., 2014). In this scenario, islet inflammation may provide a key switch for progression of the ‘benign’ autoimmunity of healthy individuals toward T1D at two levels: on T cells, by impairing peripheral immunoregulation; and on  $\beta$  cells, by increasing the overall number of pHLA-I complexes available for T-cell recognition.

## LIMITATIONS OF THIS STUDY

One limitation of our work is that the pathogenic role of the CD8<sup>+</sup> T cells recognizing the epitopes described herein remains to be definitely established. Islets from T1D patients were not available for HLA peptidomics studies, and the enrichment of these T cells in the pancreas of patients could reflect a cause or consequence of disease. It should be noted however that the same uncertainty applies to all the other islet-reactive T-cell specificities described to date. The capacity to kill  $\beta$  cells that has been described for some of them cannot be taken as conclusive evidence for their pathogenic role, since T-cell clones obtained from T1D and healthy donors kill  $\beta$  cells to a similar extent (Culina et al., 2018). Nonetheless, we here provide two key findings. First, that these epitopes are naturally processed and presented by  $\beta$  cells and are covered by the natural CD8<sup>+</sup> T-cell repertoire, hence providing potential targets for  $\beta$ -cell killing. Second, that the CD8<sup>+</sup> T cells recognizing them accumulate preferentially in the pancreas of T1D patients. This latter finding is unlikely to be serendipitous, as it did not apply to CD8<sup>+</sup> T cells recognizing the melanocyte MelanA<sub>26-35</sub> epitope, despite the fact that their frequency in the blood is ~100-fold higher than for islet epitope-reactive CD8<sup>+</sup> T cells (Culina et al., 2018).

In conclusion, the HLA-I peptidome of human  $\beta$  cells described herein provides information about the Ag processing features of  $\beta$  cells, the targets amenable to autoimmune recognition and a valuable tool for developing T-cell biomarkers and tolerogenic vaccines.

**Acknowledgements.** We thank A. Jones, K. Zehrouni, and the Diabetology nurse and medical staff of the Cochin and A. Mignot Hospital for patient recruitment; C. Maillard for technical assistance; Univercell Biosolutions for the ECN90  $\beta$ -cell line; the CyBio platform (Cochin Institute) for assistance with flow cytometry; and T. Loukanov (University of Heidelberg) for human thymi. This work was performed within the *Département Hospitalo-Universitaire* (DHU) AuthoRS and supported by the *Ile-de-France* CORDDIM and by grants from the JDRF (1-PNF-2014-155-A-V, 2-SRA-2016-164-Q-R), the *Agence Nationale de la Recherche* (ANR-2015-CE17-0018-01), the *Fondation pour la Recherche Médicale* (DEQ20140329520), the *Société Francophone du Diabète*, the *Association pour la Recherche sur le Diabète*, and the Helmsley Charitable Trust Eisenbarth nPOD Award for Team Science (2015PG-T1D052), to RM; Lilly and *Fondation Bettencourt-Schueller*, to RS; European Research Council (ERC-2012-AdG), to BK; FRFSWelbio (CR-2015A-06) and NIH-NIDDK-HIRN Consortium (1UC4DK104166-01), to DLE; and *Ile-de-France* SESAME 2010 (10022268), the City of Paris and ESPCI Paris, to JV. This project received funding from the Innovative Medicines Initiative 2 Joint Undertaking (INNODIA, 115797), which receives support from the EU Horizon 2020 program, the European Federation of Pharmaceutical Industries and Associations, JDRF and the Helmsley Charitable Trust. This research was supported by nPOD, a collaborative T1D research project funded by JDRF. Organ Procurement Organizations partnering with nPOD are listed at [www.jdrfnpod.org/our-partners.php](http://www.jdrfnpod.org/our-partners.php).

**Author contributions.** Conceptualization, D.L.E., R.M.; Methodology, S.G.D., M.E.A., M.L.C., G.A., J.V.T., A.C., A.I.L., F.D., Y.V., J.V., R.M.; Software, S.G.D.; Investigation, S.G.D., M.E.A., M.L.C., G.A., J.V.T., L.N., A.I.L., G.S., A.C., S.P., S.C., N.C., L.M.S., S.Y., F.D., D.L.E., Y.V., J.V., R.M.; Resources, S.P., M.B., P.M., M.A., M.D., B.K., L.M.S., S.B., D.D.L., E.L., J.P.B., G.B., R.S.; Data Curation, S.G.D., M.L.C., J.V.T., D.L.E., Y.V., J.V.,

R.M.; Writing – Original Draft, D.L.E., Y.V., R.M.; Writing – Review & Editing, S.G.D., S.Y., M.L.C., D.L.E., Y.V., J.V., R.M.; Visualization, S.G.D., M.E.A., M.L.C., G.A., J.V.T., L.N., G.S., Y.V., R.M.; Supervision, B.K., F.D., D.L.E., Y.V., J.V., R.M.; Funding Acquisition, S.P., B.K., S.Y., D.L.E., J.V., R.M.

**Declaration of Interests.** Some peptide sequences described herein are covered by pending patents filed by Inserm Transfert.

## REFERENCES

- Alanio, C., Lemaitre, F., Law, H.K., Hasan, M., and Albert, M.L. (2010). Enumeration of human antigen-specific naive CD8<sup>+</sup> T cells reveals conserved precursor frequencies. *Blood* *115*, 3718-3725.
- Anton, L.C., and Yewdell, J.W. (2014). Translating DRiPs: MHC class I immunosurveillance of pathogens and tumors. *J. Leukoc. Biol.* *95*, 551-562.
- Babon, J.A., DeNicola, M.E., Blodgett, D.M., Crevecoeur, I., Buttrick, T.S., Maehr, R., Bottino, R., Naji, A., Kaddis, J., Elyaman, W., et al. (2016). Analysis of self-antigen specificity of islet-infiltrating T cells from human donors with type 1 diabetes. *Nat. Med.* *22*, 1482-1487.
- Bartolomucci, A., Possenti, R., Mahata, S.K., Fischer-Colbrie, R., Loh, Y.P., and Salton, S.R. (2011). The extended granin family: structure, function, and biomedical implications. *Endocr. Rev.* *32*, 755-797.
- Bassani-Sternberg, M., Pletscher-Frankild, S., Jensen, L.J., and Mann, M. (2015). Mass spectrometry of human leukocyte antigen class I peptidomes reveals strong effects of protein abundance and turnover on antigen presentation. *Mol. Cell. Proteomics* *14*, 658-673.
- Berkers, C.R., de Jong, A., Schuurman, K.G., Linnemann, C., Meiring, H.D., Janssen, L., Neefjes, J.J., Schumacher, T.N., Rodenko, B., and Ovaa, H. (2015). Definition of proteasomal peptide splicing rules for high-efficiency spliced peptide presentation by MHC Class I molecules. *J. Immunol.* *195*, 4085-4095.
- Caron, E., Espona, L., Kowalewski, D.J., Schuster, H., Ternette, N., Alpizar, A., Schittenhelm, R.B., Ramarathnam, S.H., Lindestam Arlehamn, C.S., Chiek Koh, C., et al. (2015). An open-source computational and data resource to analyze digital maps of immunopeptidomes. *eLife* *4*.
- Coppieters, K.T., Dotta, F., Amirian, N., Campbell, P.D., Kay, T.W., Atkinson, M.A., Roep, B.O., and von Herrath, M.G. (2012). Demonstration of islet-autoreactive CD8 T cells in insulinitic lesions from recent onset and long-term type 1 diabetes patients. *J. Exp. Med.* *209*, 51-60.
- Culina, S., Lalanne, A.I., Afonso, G., Cerosaletti, K., Pinto, S., Sebastiani, G., Kuranda, K., Nigi, L., Eugster, A., Osterbye, T., et al. (2018). Islet-reactive CD8<sup>+</sup> T cell frequencies in the pancreas, but not in blood, distinguish type 1 diabetic patients from healthy donors. *Sci Immunol* *3*, eaao4013.
- Delong, T., Wiles, T.A., Baker, R.L., Bradley, B., Barbour, G., Reisdorph, R., Armstrong, M., Powell, R.L., Reisdorph, N., Kumar, N., et al. (2016). Pathogenic CD4 T cells in type 1 diabetes recognize epitopes formed by peptide fusion. *Science* *351*, 711-714.
- Dudek, N.L., Tan, C.T., Gorasia, D.G., Croft, N.P., Illing, P.T., and Purcell, A.W. (2012). Constitutive and inflammatory immunopeptidome of pancreatic beta-cells. *Diabetes* *61*, 3018-3025.
- Eizirik, D.L., Colli, M.L., and Ortis, F. (2009). The role of inflammation in insulinitis and beta-cell loss in type 1 diabetes. *Nat. Rev. Endocrinol.* *5*, 219-226.
- Eizirik, D.L., Sammeth, M., Bouckennooghe, T., Bottu, G., Sisino, G., Igoillo-Esteve, M., Ortis, F., Santin, I., Colli, M.L., Barthson, J., et al. (2012). The human pancreatic islet transcriptome: expression of candidate genes for type 1 diabetes and the impact of pro-inflammatory cytokines. *PLoS Genet.* *8*, e1002552.
- El Hage, F., Stroobant, V., Vergnon, I., Baurain, J.F., Echchakir, H., Lazar, V., Chouaib, S., Coulie, P.G., and Mami-Chouaib, F. (2008). Preprocalcitonin signal peptide generates a cytotoxic T lymphocyte-defined tumor epitope processed by a proteasome-independent pathway. *Proc. Natl. Acad. Sci. U.S.A.* *105*, 10119-10124.

Goginashvili, A., Zhang, Z., Erbs, E., Spiegelhalter, C., Kessler, P., Mihlan, M., Pasquier, A., Krupina, K., Schieber, N., Cinque, L., et al. (2015). Insulin granules. Insulin secretory granules control autophagy in pancreatic beta cells. *Science* 347, 878-882.

Gubin, M.M., Zhang, X., Schuster, H., Caron, E., Ward, J.P., Noguchi, T., Ivanova, Y., Hundal, J., Arthur, C.D., Krebber, W.J., et al. (2014). Checkpoint blockade cancer immunotherapy targets tumour-specific mutant antigens. *Nature* 515, 577-581.

James, E.A., Abreu, J.R.F., McGinty, J.W., Odegard, J.M., Fillie, Y.E., Hocter, C.N., Culina, S., Ladell, K., Price, D.A., Alkanani, A., et al. (2018). Combinatorial detection of autoreactive CD8+ T cells with HLA-A2 multimers: a multi-centre study by the Immunology of Diabetes Society T Cell Workshop. *Diabetologia* 61, 658-670.

Kracht, M.J., van Lummel, M., Nikolic, T., Joosten, A.M., Laban, S., van der Slik, A.R., van Veelen, P.A., Carlotti, F., de Koning, E.J., Hoeben, R.C., et al. (2017). Autoimmunity against a defective ribosomal insulin gene product in type 1 diabetes. *Nat. Med.* 23, 501-507.

Li, Y., Zhou, L., Li, Y., Zhang, J., Guo, B., Meng, G., Chen, X., Zheng, Q., Zhang, L., Zhang, M., et al. (2015). Identification of autoreactive CD8+ T cell responses targeting chromogranin A in humanized NOD mice and type 1 diabetes patients. *Clin. Immunol.* 159, 63-71.

Liepe, J., Marino, F., Sidney, J., Jeko, A., Bunting, D.E., Sette, A., Kloetzel, P.M., Stumpf, M.P., Heck, A.J., and Mishto, M. (2016). A large fraction of HLA class I ligands are proteasome-generated spliced peptides. *Science* 354, 354-358.

Mallone, R., Martinuzzi, E., Blancou, P., Novelli, G., Afonso, G., Dolz, M., Bruno, G., Chaillous, L., Chatenoud, L., Bach, J.M., et al. (2007). CD8+ T-cell responses identify beta-cell autoimmunity in human type 1 diabetes. *Diabetes* 56, 613-621.

Marroqui, L., Dos Santos, R.S., Floyel, T., Grieco, F.A., Santin, I., Op de Beeck, A., Marselli, L., Marchetti, P., Pociot, F., and Eizirik, D.L. (2015). TYK2, a candidate gene for type 1 diabetes, modulates apoptosis and the innate immune response in human pancreatic beta-cells. *Diabetes* 64, 3808-3817.

Marroqui, L., Dos Santos, R.S., Op de Beeck, A., Coomans de Brachene, A., Marselli, L., Marchetti, P., and Eizirik, D.L. (2017). Interferon-alpha mediates human beta cell HLA class I overexpression, endoplasmic reticulum stress and apoptosis, three hallmarks of early human type 1 diabetes. *Diabetologia* 60, 656-667.

Marroqui, L., Santin, I., Dos Santos, R.S., Marselli, L., Marchetti, P., and Eizirik, D.L. (2014). BACH2, a candidate risk gene for type 1 diabetes, regulates apoptosis in pancreatic beta-cells via JNK1 modulation and crosstalk with the candidate gene PTPN2. *Diabetes* 63, 2516-2527.

Martinuzzi, E., Novelli, G., Scotto, M., Blancou, P., Bach, J.M., Chaillous, L., Bruno, G., Chatenoud, L., van, E.P., and Mallone, R. (2008). The frequency and immunodominance of islet-specific CD8+ T-cell responses change after type 1 diabetes diagnosis and treatment. *Diabetes* 57, 1312-1320.

Mbikay, M., Seidah, N.G., and Chretien, M. (2001). Neuroendocrine secretory protein 7B2: structure, expression and functions. *Biochem. J.* 357, 329-342.

McGinty, J.W., Chow, I.T., Greenbaum, C., Odegard, J., Kwok, W.W., and James, E.A. (2014). Recognition of post-translationally modified glutamic acid decarboxylase 65 epitopes in subjects with type 1 diabetes. *Diabetes* 63, 3033-3040.

Montgomery, S.B., Sammeth, M., Gutierrez-Arcelus, M., Lach, R.P., Ingle, C., Nisbett, J., Guigo, R., and Dermitzakis, E.T. (2010). Transcriptome genetics using second generation sequencing in a Caucasian population. *Nature* 464, 773-777.

Moore, F., Colli, M.L., Cnop, M., Esteve, M.I., Cardozo, A.K., Cunha, D.A., Bugliani, M., Marchetti, P., and Eizirik, D.L. (2009). PTPN2, a candidate gene for type 1 diabetes, modulates interferon-gamma-induced pancreatic beta-cell apoptosis. *Diabetes* 58, 1283-1291.

Nejentsev, S., Howson, J.M., Walker, N.M., Szeszko, J., Field, S.F., Stevens, H.E., Reynolds, P., Hardy, M., King, E., Masters, J., et al. (2007). Localization of type 1 diabetes susceptibility to the MHC class I genes HLA-B and HLA-A. *Nature* 450, 887-892.

Ortis, F., Naamane, N., Flamez, D., Ladriere, L., Moore, F., Cunha, D.A., Colli, M.L., Thykjaer, T., Thorsen, K., Orntoft, T.F., et al. (2010). Cytokines interleukin-1beta and tumor necrosis factor-alpha regulate different transcriptional and alternative splicing networks in primary beta-cells. *Diabetes* 59, 358-374.

Pinto, S., Sommermeyer, D., Michel, C., Wilde, S., Schendel, D., Uckert, W., Blankenstein, T., and Kyewski, B. (2014). Misinitiation of intrathymic MART-1 transcription and biased TCR usage explain the high frequency of MART-1-specific T cells. *Eur. J. Immunol.* 44, 2811-2821.

Ravassard, P., Hazhouz, Y., Pechberty, S., Bricout-Neveu, E., Armanet, M., Czernichow, P., and Scharfmann, R. (2011). A genetically engineered human pancreatic beta cell line exhibiting glucose-inducible insulin secretion. *J. Clin. Invest.* 121, 3589-3597.

Rondas, D., Crevecoeur, I., D'Hertog, W., Bomfim Ferreira, G., Staes, A., Garg, A.D., Eizirik, D.L., Agostinis, P., Gevaert, K., Overbergh, L., et al. (2015). Citrullinated glucose-regulated protein 78 is an autoantigen in type 1 diabetes. *Diabetes* 64, 573-586.

Scotto, M., Afonso, G., Larger, E., Raverdy, C., Lemonnier, F.A., Carel, J.C., Dubois-Laforgue, D., Baz, B., Levy, D., Gautier, J.F., et al. (2012). Zinc transporter (ZnT)8(186-194) is an immunodominant CD8+ T cell epitope in HLA-A2+ type 1 diabetic patients. *Diabetologia* 55, 2026-2031.

Skowera, A., Ellis, R.J., Varela-Calvino, R., Arif, S., Huang, G.C., Van-Krinks, C., Zaremba, A., Rackham, C., Allen, J.S., Tree, T.I., et al. (2008). CTLs are targeted to kill beta cells in patients with type 1 diabetes through recognition of a glucose-regulated preproinsulin epitope. *J. Clin. Invest.* 118, 3390-3402.

Standifer, N.E., Ouyang, Q., Panagiotopoulos, C., Verchere, C.B., Tan, R., Greenbaum, C.J., Pihoker, C., and Nepom, G.T. (2006). Identification of novel HLA-A\*0201-restricted epitopes in recent-onset type 1 diabetic subjects and antibody-positive relatives. *Diabetes* 55, 3061-3067.

Villate, O., Turatsinze, J.V., Mascali, L.G., Grieco, F.A., Nogueira, T.C., Cunha, D.A., Nardelli, T.R., Sammeth, M., Salunkhe, V.A., Esguerra, J.L., et al. (2014). Nova1 is a master regulator of alternative splicing in pancreatic beta cells. *Nucleic Acids Res.* 42, 11818-11830.

Weckman, A., Di Ieva, A., Rotondo, F., Syro, L.V., Ortiz, L.D., Kovacs, K., and Cusimano, M.D. (2014). Autophagy in the endocrine glands. *J. Mol. Endocrinol.* 52, R151-163.



## FIGURES

### **Figure 1. The HLA-I peptidome of human $\beta$ cells is enriched by cytokine exposure and displays the expected amino-acid length and motifs.**

(A) HLA-I expression detected by flow cytometry on ECN90  $\beta$  cells under basal (red), IFN- $\gamma$ -stimulated (blue) and IFN- $\gamma$ /TNF- $\alpha$ /IL-1 $\beta$ -stimulated conditions (green). The grey profile displays IFN- $\gamma$ /TNF- $\alpha$ /IL-1 $\beta$ -stimulated cells stained with an isotype control monoclonal antibody (mAb; the identical profiles of basal and IFN- $\gamma$ -stimulated conditions are not shown). (B) HLA-I heavy chain expression detected by Western blot on the same cell aliquots, with  $\alpha$ -tubulin bands shown as loading control. (C) aa length of the 2,997 peptides detected in  $\geq 2$  out of 5 biological replicates. (D) Sequence logo plots displaying the HLA-A2 (top), -A3 (middle) and -B40/B49 (bottom) binding motifs for the 3 major Gibbs clusters. The X-axis shows the residue position within nonamer peptide sequences. The Y-axis shows the information content, with the size of each aa symbol proportional to its frequency. (E) Heat map of the predicted HLA-I binding affinities of nonamer peptides. Each column represents a unique peptide. Red, green and grey shades indicate high binders ( $K_D \leq 50$  nM), low binders ( $K_D \leq 2,000$  nM) and non-binders ( $K_D > 2,000$  nM), respectively. (F) Number of peptides identified in ECN90  $\beta$  cells.  $**p=0.008$  and  $*p=0.02$  by Mann-Whitney test. (G) The bioinformatics analysis pipeline used (see STAR methods for details). The 3,544 peptides identified were first filtered based on inter-sample reproducibility ( $n=2,997$ ) and aa length ( $n=2,795$ ). From this dataset, we identified 217 peptides derived from ubiquitous proteins carrying PTMs (blue), from which 99 (Table S2) were enriched in HLA-I-purified samples; and 15 peptide splice variants (brown; see Fig. S1 for the identification strategy), from which 10 were enriched in HLA-I-purified samples. The remaining  $\beta$ -cell-enriched peptides (both conventional and with PTMs; red) were filtered based on non-ubiquitous expression ( $n=411$ ),  $\beta$ -cell-enriched expression ( $n=139$ ) and enrichment in HLA-I-purified samples ( $n=86$ ; Table S1). Finally, mRNA splice variants

(green, n=2) were identified by searching the HLA-I peptidomics dataset against the predicted aa neo-sequences obtained from RNAseq analysis. For this RNAseq pipeline (dashed boxes), 53,280 mRNAs were filtered based on islet mRNA expression (n=14,504), low mTEC mRNA expression (n=908), islet enrichment compared to control tissues (n=166) and generation of a predicted aa neo-sequence (n=88). The 336 predicted aa neo-sequences obtained from these 88 mRNA variants were analyzed in parallel for the presence of predicted HLA-2 binders (n=66) with a 9-10-aa length (n=43) and a neo-sequence of  $\geq 3$  aa (n=39). The indicated epitope candidates were further filtered on predicted and experimental HLA-A2 binding to focus subsequent CD8<sup>+</sup> T-cell recognition studies on HLA-A2-restricted peptides (see text).

**Figure 2. pHLA-I complexes of human  $\beta$  cells are enriched in peptides derived from secretory granule proteins, including known PPI epitopes.** (A) Number of peptides (n=86 from  $\beta$ -cell-enriched proteins, n=10 transpeptidation products, n=2 mRNA splice products) identified in ECN90  $\beta$  cells after bioinformatics filtering (Fig. 1G). (B) Source proteins of the 98 peptides (detailed in Table S1). (C) Mapping of HLA-A2-restricted PPI peptides identified in ECN90  $\beta$  cells. PTM variants (see Table S1) and a PPI<sub>15-26</sub> length variant (in italics) were also identified. (D) Origin of the 42 proteins yielding the 98 peptides identified in ECN90  $\beta$  cells, including splice peptides generated from IAPP and NPY. (E) Predicted HLA-I restrictions of the same peptides. (F) Source proteins of the 33 peptides (Table S3) identified in HLA-A2<sup>+</sup> primary human islets. Asterisks indicate proteins for which some peptides identified were identical or length variants compared to those identified in ECN90  $\beta$  cells, including the identical IAPP<sub>15-17/5-10</sub> splice peptide. Exploded slices indicate source proteins not identified in ECN90  $\beta$  cells. (G) HLA-I heavy chain expression detected by Western blot on primary islets and ECN90  $\beta$  cells under basal and IFN- $\gamma$ /TNF- $\alpha$ /IL-1 $\beta$ -stimulated

conditions, with  $\beta$ -actin bands shown as loading control. A representative islet preparation out of 3 analyzed is shown.

**Figure 3. Gating strategy for the combinatorial analysis of  $\beta$ -cell peptide MMr<sup>+</sup>CD8<sup>+</sup> T cells in T1D and healthy subjects.** (A) Frozen-thawed peripheral blood mononuclear cells (PBMCs) from T1D donor D314D were magnetically depleted of CD8<sup>-</sup> cells before staining, acquisition and analysis (see STAR Methods). Cells were sequentially gated on small lymphocytes, singlets, live cells (Live/Dead Aqua<sup>-</sup>), CD3<sup>+</sup>CD8<sup>+</sup> T cells and total PE<sup>+</sup>, PE-CF594<sup>+</sup>, APC<sup>+</sup>, BV650<sup>+</sup>, BV711<sup>+</sup> and BV786<sup>+</sup> MMr<sup>+</sup> T cells. Using Boolean operators, these latter gates allowed to selectively visualize each double-MMr<sup>+</sup> population by including only those events positive for the corresponding fluorochrome pair. (B-C) The final readout obtained for T1D donor D314D (B) and healthy donor H170S (C) is shown for the 15 peptides analyzed. Events corresponding to each epitope-reactive population are overlaid in different colors within each plot, with MMr<sup>-</sup> events overlaid in light grey. The small dot plots on the right of each panel depict CD45RA (x-axis) and CCR7 (y-axis) expression in the corresponding MMr<sup>+</sup> fraction. Numbers in each panel indicate the MMr<sup>+</sup>CD8<sup>+</sup> T-cell frequency out of total CD8<sup>+</sup> T cells and the percent naïve (CD45RA<sup>+</sup>CCR7<sup>+</sup>) fraction among MMr<sup>+</sup> cells.

**Figure 4. HLA-A2-restricted  $\beta$ -cell peptides are targeted by a circulating naïve CD8<sup>+</sup> T-cell repertoire in healthy donors.** MMr<sup>+</sup>CD8<sup>+</sup> cells reactive to HLA-A2-binding  $\beta$ -cell peptides (Fig. S2) were stained *ex vivo* from PBMCs of 5-6 HLA-A2<sup>+</sup> healthy donors (Table S4). (A-F) Representative dot plots of different MMr staining patterns: high frequency, clustered pattern (A; CCNI-008<sub>14-22</sub>); intermediate frequency, clustered pattern (B; SCG5<sub>186-195</sub>); low frequency, clustered pattern (C; CHGB<sub>440-448</sub>); high frequency, spread pattern (D;

LARP4-006<sub>214-222</sub>); and the  $\beta$ -cell PPI<sub>6-14</sub> (E) and viral Flu MP<sub>58-66</sub> (F) positive controls. (**G-H**) MMr<sup>+</sup>CD8<sup>+</sup> cells reactive to  $\beta$ -cell peptides identified in HLA-I peptidomics (G) and RNAseq (H) pipelines. PPI<sub>6-14</sub> and Flu MP<sub>58-66</sub> peptides were included as controls. Frequencies out of total CD8<sup>+</sup> T cells are depicted. Dotted lines indicate the expected frequency of naïve MMr<sup>+</sup>CD8<sup>+</sup> T cells, bars show median values. The 20  $\beta$ -cell peptides displaying the expected CD8<sup>+</sup> T-cell frequency and a clustered MMr staining pattern were retained and are marked with an asterisk (2 asterisks for the 13 peptides further analyzed).  $\beta$ -cell peptides in italics were excluded despite their cognate MMr<sup>+</sup>CD8<sup>+</sup> T-cell frequencies because of their spread MMr staining pattern. At least  $0.6 \times 10^6$  CD8<sup>+</sup> T cells were counted for each donor (median  $1.4 \times 10^6$ , range  $0.6-4.9 \times 10^6$ ). (**I-J**) Percent Ag-experienced cells (CD45RA<sup>-</sup>CCR7<sup>-</sup>, CD45RA<sup>+</sup>CCR7<sup>-</sup> and CD45RA<sup>-</sup>CCR7<sup>+</sup>) out of total MMr<sup>+</sup> cells for the  $\beta$ -cell peptides depicted in panels G-H, respectively. Data points with <5 MMr<sup>+</sup> cells were excluded from this analysis (median 19 MMr<sup>+</sup> cells, range 5-808 for  $\beta$ -cell peptides). NA, not available.

**Figure 5. Circulating CD8<sup>+</sup> T cells reactive to HLA-A2-restricted  $\beta$ -cell peptides display similar *ex-vivo* frequencies and a predominantly naïve phenotype in T1D and healthy subjects.** (**A**) Frequencies of MMr<sup>+</sup>CD8<sup>+</sup> cells reactive to the indicated  $\beta$ -cell peptides in T1D (grey; n=10) and healthy subjects (white; n=10; donors listed in Table S4). PPI<sub>6-14</sub> and Flu MP<sub>58-66</sub> peptides were included as controls. At least  $0.6 \times 10^6$  CD8<sup>+</sup> T cells were counted for each donor (median  $1.0 \times 10^6$ , range  $0.6-2.4 \times 10^6$ ). (**B**) Percent Ag-experienced cells out of total MMr<sup>+</sup> cells for the  $\beta$ -cell peptides depicted in panel A. Data points with <5 MMr<sup>+</sup> cells were excluded (median 14 MMr<sup>+</sup> cells, range 5-160 for  $\beta$ -cell peptides). Bars show median values. NA, not available.

**Fig. 6. Pancreas-infiltrating cells reactive to the HLA-A2-restricted IAPP<sub>15-17/5-10</sub>, ISL1<sub>276-284</sub> and UCN3<sub>1-9</sub> peptides are enriched in T1D patients.** Pancreas sections from nPOD cases (Table S5) were immunohistochemically stained *in situ* with MMrs loaded with IAPP<sub>15-17/5-10</sub>, ISL1<sub>276-284</sub>, UCN3<sub>1-9</sub> (selected from Fig. S3), positive control ZnT8<sub>186-194</sub> and negative control melanocyte MelanA<sub>26-35</sub> peptide. **(A-D, I-L, Q-R)** Representative pancreas images (20X magnification; scale bar 100  $\mu$ m). **(E-H, M-P)** Higher magnification of the dotted areas highlighted on the left of each panel (scale bar 40  $\mu$ m for panels E, M; 38  $\mu$ m for F, N; 45  $\mu$ m for G, O; 36  $\mu$ m for H, P). **(S-T)** Number of MMr<sup>+</sup> cells/mm<sup>2</sup> section area of pancreas (S) and PLNs (T). Each point represents an individual case, bars indicate median values. \*P  $\leq$  0.05 and \*\*P  $\leq$  0.009 by Mann-Whitney test. NA, not assessed. **(U-W)** Fluorescent confocal microscopy on pancreas sections from T1D EUnPOD case #060217 for CD8 (green), CD45RO (blue) and pooled IAPP<sub>15-17/5-10</sub>/ISL1<sub>276-284</sub>/UCN3<sub>1-9</sub> MMrs (red). Examples of CD8<sup>+</sup>CD45RO<sup>-</sup>MMr<sup>-</sup>, CD8<sup>+</sup>CD45RO<sup>+</sup>MMr<sup>-</sup> and CD8<sup>+</sup>CD45RO<sup>+</sup>MMr<sup>+</sup> cells are shown in panel U (scale bar 25  $\mu$ m), V and W (scale bar 10  $\mu$ m), respectively.

## TABLES

**Table 1. Summary of  $\beta$ -cell peptides tested for recognition by circulating naïve CD8<sup>+</sup> T cells of healthy subjects.** The peptides presented in Fig. 4 are alphabetically listed and classified according to type (conventional, peptide splice and mRNA splice). The corresponding median RPKM values detected in islets (control- and cytokine-treated) and mTECs (HLA Class II<sup>hi</sup> and Class II<sup>lo</sup>) are shown. For proteins not arising from alternative mRNA splicing, RPKM values refer to the most prevalent islet mRNA isoform coding for the corresponding peptide. Subsequent columns detail the number of T-cell<sup>+</sup> donors ( $\geq 5/10^7$  MMr<sup>+</sup> cells counted), the median MMr<sup>+</sup> frequency, the median percent Ag-experienced cells within the MMr<sup>+</sup> fraction (for peptides/donors with  $\geq 5$  MMr<sup>+</sup> cells), the number of donors with  $\geq 5$  MMr<sup>+</sup> cells, the MMr staining pattern (clustered, spread or not detected, ND) and the final validation outcome. The 20 validated  $\beta$ -cell peptides (in bold) displayed the expected CD8<sup>+</sup> T-cell frequency and a clustered MMr staining pattern and are marked with an asterisk (2 asterisks for the 13 peptides further analyzed). NA, not available.

Protein or mRNA	Peptide	Sequence	Type	Islet RPKM, control	Islet RPKM, cytokines	mTEC RPKM, HLA-II <sup>hi</sup>	mTEC RPKM, HLA-II <sup>lo</sup>	T-cell <sup>+</sup> donors	Frequency among CD8 <sup>+</sup> cells	% Ag experienced	Donors with ≥5 MMr <sup>+</sup> cells	MMr staining pattern	Validation
ACLY-004	70-78	GLVGVNLT	mRNA splice	22.5	5.7	0.0	0.0	0/6	0.00E+00	NA	0/6	ND	No
C15orf48-003	73-81	FLLQNPCPL	mRNA splice	9.8	18.1	0.0	0.0	0/6	8.30E-08	29	1/6	Spread	No
C16orf70-010	44-53	VLYSEQVIEV	mRNA splice	0.7	12.3	0.0	0.0	0/6	2.54E-07	14	1/6	Spread	No
CCNI-008	11-19	ILDKLNWDL	mRNA splice	41.0	25.9	0.4	0.3	1/6	1.05E-07	20	1/6	Spread	No
<b>**CCNI-008</b>	<b>14-22</b>	<b>KLNWDLHTA</b>	<b>mRNA splice</b>	<b>41.0</b>	<b>25.9</b>	<b>0.4</b>	<b>0.3</b>	<b>4/6</b>	<b>5.05E-06</b>	<b>10</b>	<b>6/6</b>	<b>Clustered</b>	<b>Yes</b>
CCNI-008	53-61	SLPLNSVYV	mRNA splice	41.0	25.9	0.4	0.3	1/6	5.20E-08	NA	0/6	Spread	No
<b>*CHGA</b>	<b>344-352</b>	<b>KMDQLAKEL</b>	<b>Conventional</b>	<b>587.2</b>	<b>1881.9</b>	<b>7.9</b>	<b>13.2</b>	<b>3/6</b>	<b>9.75E-07</b>	<b>18</b>	<b>5/6</b>	<b>Clustered</b>	<b>Yes</b>
CHGA	402-411	SLEAGLPLQV	Conventional	587.2	1881.9	7.9	13.2	0/6	1.66E-07	NA	0/6	Spread	No
CHGB	440-448	FLGEGHHRV	Conventional	1212.4	935.2	9.6	18.4	1/6	6.67E-07	28	4/6	Clustered	No
CLDN7-008	60-68	GMMSCKIGL	mRNA splice	20.8	17.5	0.0	0.1	0/6	0.00E+00	NA	0/6	ND	No
FAM171B	19-28	VLLKARLVPA	Conventional	4.3	4.0	6.5	5.0	3/6	1.70E-06	7	5/6	Spread	No
<b>**GAD2-003</b>	<b>179-187</b>	<b>KIIKLFFRL</b>	<b>mRNA splice</b>	<b>22.2</b>	<b>21.2</b>	<b>0.0</b>	<b>0.0</b>	<b>5/6</b>	<b>5.14E-06</b>	<b>19</b>	<b>6/6</b>	<b>Clustered</b>	<b>Yes</b>
GNAS-002	31-39	ALLWLSCSI	mRNA splice	256.1	123.2	0.6	0.0	0/6	4.92E-07	30	2/6	Clustered	No
GNAS-002	32-41	LLWLSCSIAL	mRNA splice	256.1	123.2	0.6	0.0	0/6	0.00E+00	NA	0/6	ND	No
GNAS-002	34-42	WLSCSIAL	mRNA splice	256.1	123.2	0.6	0.0	1/6	3.16E-07	23	2/6	Clustered	No
<b>**GNAS-036</b>	<b>67-75</b>	<b>YMCTHRLLL</b>	<b>mRNA splice</b>	<b>48.9</b>	<b>45.1</b>	<b>0.0</b>	<b>0.0</b>	<b>4/6</b>	<b>1.25E-06</b>	<b>9</b>	<b>5/6</b>	<b>Clustered</b>	<b>Yes</b>
GNAS-036	67-76	YMCTHRLLLL	mRNA splice	48.9	45.1	0.0	0.0	0/6	0.00E+00	NA	0/6	ND	No
<b>**GNAS-036</b>	<b>124-132</b>	<b>AMSNLVPPV</b>	<b>mRNA splice</b>	<b>48.9</b>	<b>45.1</b>	<b>0.0</b>	<b>0.0</b>	<b>5/6</b>	<b>1.30E-06</b>	<b>14</b>	<b>5/6</b>	<b>Clustered</b>	<b>Yes</b>
GNAS-036	185-194	QLIDCAQYFL	mRNA splice	48.9	45.1	0.0	0.0	0/6	4.76E-08	NA	0/6	ND	No
GPR119	48-56	AVADTLIGV	Conventional	9.4	7.4	0.0	0.0	0/6	1.26E-07	NA	0/6	Spread	No
<b>**IAPP/IAPP</b>	<b>15-17/5-10</b>	<b>VALKLQVFL</b>	<b>Peptide splice</b>	<b>1257.1</b>	<b>392.4</b>	<b>0.3</b>	<b>0.0</b>	<b>1/6</b>	<b>2.45E-07</b>	<b>9</b>	<b>1/6</b>	<b>Clustered</b>	<b>Yes</b>
<b>**IAPP-002</b>	<b>33-42</b>	<b>VLSRNILLEL</b>	<b>mRNA splice</b>	<b>74.0</b>	<b>24.3</b>	<b>0.0</b>	<b>0.0</b>	<b>3/6</b>	<b>9.63E-07</b>	<b>35</b>	<b>4/6</b>	<b>Clustered</b>	<b>Yes</b>
IAPP-004	9-18	CLDQIIFTV	mRNA splice	609.8	257.1	0.0	0.0	1/6	2.59E-07	37	2/6	Clustered	No
IGF2BP3	552-560	KIQEILTQV	Conventional	0.2	0.4	5.3	0.9	0/5	2.66E-07	24	4/5	Spread	No

<b>**ISL1</b>	<b>276-284</b>	<b>GLQANPVEV</b>	<b>Conventional</b>	<b>26.2</b>	<b>27.9</b>	<b>17.0</b>	<b>26.9</b>	<b>3/6</b>	<b>1.83E-06</b>	<b>26</b>	<b>3/6</b>	<b>Clustered</b>	<b>Yes</b>
<b>*KCNK16</b>	<b>129-137</b>	<b>ALLGIPLNV</b>	<b>Conventional</b>	33.3	22.5	0.0	0.0	<b>5/6</b>	<b>4.44E-06</b>	13	<b>6/6</b>	<b>Clustered</b>	<b>Yes</b>
KCNK16-002	234-242	SLAAIWILL	mRNA splice	33.3	22.5	0.0	0.0	0/6	4.37E-08	NA	0/6	ND	No
KCNK16-002	240-248	ILLGLAWLA	mRNA splice	33.3	22.5	0.0	0.0	0/6	1.30E-07	NA	0/6	Spread	No
<b>*KIF1A</b>	<b>1347-1355</b>	<b>VLDTSVAYV</b>	<b>Conventional</b>	<b>19.5</b>	<b>17.7</b>	<b>1.0</b>	<b>1.9</b>	<b>3/6</b>	<b>2.25E-06</b>	<b>33</b>	<b>5/6</b>	<b>Clustered</b>	<b>Yes</b>
KIF1A	1480-1488	KLSEMSVTL	Conventional	19.5	17.7	1.0	1.9	0/5	5.2E-07	18.2	5/5	Spread	No
LARP4-006	214-222	RLMDSSIYS	mRNA splice	6.8	10.5	0.0	0.0	2/6	8.95E-07	20	4/6	Spread	No
LARP4-006	355-363	YLQKETSTL	mRNA splice	6.8	10.5	0.0	0.0	2/6	7.94E-07	21	5/6	Spread	No
LGMN-012	68-76	VMINPTPGI	mRNA splice	0.0	10.9	0.0	0.0	0/6	0.00E+00	NA	0/6	ND	No
PCSK1-002	8-17	FLFFSQIGSL	mRNA splice	16.2	13.8	0.0	0.0	0/6	0.00E+00	NA	0/6	ND	No
<b>**PCSK2</b>	<b>30-38</b>	<b>FTNHFLVEL</b>	<b>Conventional</b>	<b>73.2</b>	<b>43.4</b>	<b>0.7</b>	<b>0.0</b>	<b>4/6</b>	<b>1.25E-06</b>	<b>9</b>	<b>6/6</b>	<b>Clustered</b>	<b>Yes</b>
PCSK2-001	11-19	AAAGFLFCV	mRNA splice	36.5	17.8	0.0	0.1	2/6	5.40E-07	23	2/6	Spread	No
PCSK2-001	15-23	FLFCVMVFA	mRNA splice	36.5	17.8	0.0	0.1	2/6	3.79E-07	54	2/6	Spread	No
PDXDC1-013	174-183	YLCNQDVAFL	mRNA splice	13.5	0.8	0.0	0.0	2/6	6.21E-07	17	3/6	Spread	No
PIK3R3	144-152	SLAQYNPKL	Conventional	2.2	2.4	18.7	9.2	3/6	8.50E-07	12	4/6	Spread	No
PRPH	171-179	GLAEDLAAL	Conventional	4.0	3.8	1.1	0.5	3/6	1.08E-06	19	5/6	Spread	No
<b>*PTPRN-021</b>	<b>392-402</b>	<b>SLAAGVKLEI</b>	<b>mRNA splice</b>	<b>81.5</b>	<b>98.3</b>	<b>0.0</b>	<b>0.0</b>	<b>5/5</b>	<b>4.49E-06</b>	<b>17</b>	<b>5/5</b>	<b>Clustered</b>	<b>Yes</b>
<b>*PTPRN-021</b>	<b>398-407</b>	<b>KLLEILAEHV</b>	<b>mRNA splice</b>	<b>81.5</b>	<b>98.3</b>	<b>0.0</b>	<b>0.0</b>	<b>5/5</b>	<b>4.30E-06</b>	<b>13</b>	<b>5/5</b>	<b>Clustered</b>	<b>Yes</b>
PTPRN-021	402-409	ILAEHVHM	mRNA splice	81.5	98.3	0.0	0.0	1/5	5.41E-07	9	4/5	Clustered	No
<b>**PTPRN2-005</b>	<b>11-19</b>	<b>LLLLLPPRV</b>	<b>mRNA splice</b>	<b>33.3</b>	<b>10.8</b>	<b>0.0</b>	<b>0.0</b>	<b>4/6</b>	<b>1.67E-06</b>		<b>3/6</b>	<b>Clustered</b>	<b>Yes</b>
<b>*PTPRN2-005</b>	<b>19-27</b>	<b>VLPAAPSSV</b>	<b>mRNA splice</b>	<b>33.3</b>	<b>10.8</b>	<b>0.0</b>	<b>0.0</b>	<b>6/6</b>	<b>5.53E-06</b>	<b>8</b>	<b>6/6</b>	<b>Clustered</b>	<b>Yes</b>
<b>*REX02-020</b>	<b>2-10</b>	<b>SVANALWIV</b>	<b>mRNA splice</b>	<b>4.2</b>	<b>10.5</b>	<b>0.0</b>	<b>0.0</b>	<b>5/6</b>	<b>1.94E-06</b>	<b>28</b>	<b>5/6</b>	<b>Clustered</b>	<b>Yes</b>
<b>**SCG5</b>	<b>186-195</b>	<b>YLQQQRLDNV</b>	<b>Conventional</b>	<b>252.5</b>	<b>163.2</b>	<b>3.2</b>	<b>2.9</b>	<b>5/6</b>	<b>1.16E-06</b>	<b>20</b>	<b>6/6</b>	<b>Clustered</b>	<b>Yes</b>
<b>**SCG5-009</b>	<b>186-194</b>	<b>FLSGAVNRL</b>	<b>mRNA splice</b>	<b>0.3</b>	<b>41.4</b>	<b>0.0</b>	<b>0.0</b>	<b>5/5</b>	<b>6.62E-06</b>	<b>7</b>	<b>5/5</b>	<b>Clustered</b>	<b>Yes</b>
<b>**SLC30A8-002</b>	<b>16-25</b>	<b>KMYAFTLESV</b>	<b>mRNA splice</b>	<b>43.1</b>	<b>38.1</b>	<b>0.3</b>	<b>0.0</b>	<b>4/6</b>	<b>1.33E-06</b>	<b>7</b>	<b>2/6</b>	<b>Clustered</b>	<b>Yes</b>
ST18	304-312	SLLEQAIAL	Conventional	8.2	4.8	0.2	0.5	<b>3/6</b>	6.70E-07	33	<b>3/6</b>	Spread	No
<b>**UCN3</b>	<b>1-9</b>	<b>MLMPVHLL</b>	<b>Conventional</b>	<b>61.9</b>	<b>26.7</b>	<b>0.2</b>	<b>0.1</b>	<b>5/5</b>	<b>1.30E-05</b>	<b>11</b>	<b>5/5</b>	<b>Clustered</b>	<b>Yes</b>
WARS-035	66-74	GLDEIDSAV	mRNA splice	0.3	31.8	0.0	0.2	0/6	3.36E-07	0	2/6	Spread	No



## **STAR METHODS**

### **Contact for reagent and resource sharing**

Further information and requests for resources and reagents should be directed to and will be fulfilled by the Lead Contact, Roberto Mallone (roberto.mallone@inserm.fr).

### **Experimental model and subject details**

#### ***Cell lines***

The ECN90 cell line (HLA-A\*02:01/03:01, -B\*40:01/49:01, -C\*03:04/07:01) was derived from a human neonatal pancreas using described protocols (Ravassard et al., 2011). Cells were seeded in 15-cm diameter tissue culture dishes (Techno Plastic Products AG) coated with 0.1% fibronectin solution from human plasma (Sigma; 400 ng/cm<sup>2</sup>) and extracellular matrix from Engelbreth-Holm-Swarm murine sarcoma (Sigma; 1-2.4 mg/cm<sup>2</sup>). They were maintained in DMEM/F12 medium supplemented with 2% bovine serum albumin, 6.7 ng/ml sodium selenite, 10 mM nicotinamide, 50  $\mu$ M  $\beta$ -mercaptoethanol and penicillin/streptomycin. IFN- $\gamma$  (R&D) was added to the cell culture at 80-90% confluence at a final concentration of 500 U/ml for 16-18 h. IFN- $\gamma$ , TNF- $\alpha$  and IL-1 $\beta$  (all from R&D) were added at a final concentration of 2,000 U/ml, 1,100 U/ml, and 1,000 U/ml, respectively.

#### ***Primary human tissues and PBMCs***

For HLA-I peptidomics experiments, transplantation-grade, undispersed primary human islets (75% purity; HLA-A\*02:01/25:01, -B\*39:01/51:01, -C\*12:03/14:02) were obtained from a brain-dead non-diabetic organ donor (age 49 years, male, BMI 37 kg/m<sup>2</sup>; protocol approved by the *Agence de la Biomédecine*) with standard procedures and maintained in CMRL 1066 medium (Sigma) supplemented with 10% fetal bovine serum. For RNAseq analyses, primary human islets from 5 brain-dead non-diabetic organ donors (mean age 50.6 $\pm$ 10.2 years, 3 females, 2 males, BMI 25 $\pm$ 2 kg/m<sup>2</sup>; 57 $\pm$ 5%  $\beta$  cells; protocol approved by the Ethics

Committee of the University of Pisa, Italy) were exposed or not to IFN- $\gamma$  (1,000 U/ml) and IL-1 $\beta$  (50 U/ml) for 48 h. For HLA-I expression analyses (Fig. 2G), primary human islets were from 3 non-diabetic organ donors (mean age 54.7 $\pm$ 14.3 years, 1 female, 2 males, BMI 29 $\pm$ 5 kg/m<sup>2</sup>; protocol approved by the Ethics Committee of the University of Pisa, Italy). Primary human HLA Class II<sup>lo</sup> and Class II<sup>hi</sup> mTECs were purified as described (Pinto et al., 2014) from the thymi of 3 children (male gender, age 6 days, 4 months and 9 months) undergoing corrective cardiac surgery at the University of Heidelberg, Germany (Ethics approval 367/2002). Blood was drawn into 9 ml sodium heparin tubes from T1D and healthy donors (Table S4) under the Ethics approval DC-2015-2536 Ile-de-France I. Informed consent was obtained from all subjects, or next-of-kin for islet donors. For *in-situ* MMr staining, pancreas and PLN sections were provided by nPOD.

## Method details

### *Purification of pHLA-I complexes*

W6/32 and HC10 anti-HLA-I mAbs were purified on a protein A Prosep Ultraplus column (Millipore) from hybridoma supernatants. The W6/32 mAb recognizes a conformational epitope formed by the interaction of the HLA-I heavy chain and  $\beta$ 2-microglobulin and was used for purifying pHLA-I complexes and for flow cytometry in conjunction with an FITC-conjugated goat anti-mouse Ig Ab (BD). The HC10 mAb recognizes a linear epitope on the HLA-I heavy chain and was used for Western blotting along with an anti- $\alpha$ -tubulin mAb for loading control (Fig. 1B). Since  $\alpha$ -tubulin expression is higher in ECN90  $\beta$  cells than in primary islets, an anti- $\beta$ -actin mAb was used for loading control to compare HLA-I expression and upregulation between the two cell types (Fig. 2G). To this end, the membrane previously probed for HLA-I (45 kD) was stripped and reprobed for  $\beta$ -actin (42 kD).

The HLA-I peptidome of the ECN90  $\beta$ -cell line was obtained from 5 biological replicates. A single biological replicate was available for primary human islets. Frozen cell pellets ( $\sim 20 \times 10^6$ /condition for ECN90 cells;  $\sim 25,000$  islet equivalents/condition for primary islets, corresponding to  $\sim 19 \times 10^6$   $\beta$  cells) were resuspended in a buffer containing 10 mM Tris-HCl pH 8.0, 150 mM NaCl, 5 mM EDTA, 0.1% (v/v) Complete Protease Inhibitor Cocktail (Roche), and 1% (w/v) octyl- $\beta$ -D glucopyranoside (Sigma). Lysis was carried out at 4°C for 1 h under rotation, with two sonication steps at 30 and 60 min. Lysates were cleared by centrifugation and pHLA-I complexes immunoaffinity-purified with the W6/32 mAb covalently bound to Protein A Sepharose CL-4B beads (GE Healthcare) by dimethyl pimelimidate cross-linking. Beads were subsequently loaded on GELoader Tips (20  $\mu$ l; ThermoFisher) and washed before elution of pHLA-I complexes with 10% acetic acid. Aliquots were collected at each washing and elution step for analysis by 12% SDS-PAGE and Western blot using the HC10 mAb to verify the yield and purity of the eluted HLA-I.

Eluted peptides and the associated HLA-I heavy chain and  $\beta$ 2-microglobulin obtained from  $20 \times 10^6$  cells were concentrated to 20  $\mu$ l by vacuum centrifugation, acidified with 10  $\mu$ l of 1% formic acid (Normapur) and loaded on C18 stage tips (ThermoFisher) prewashed with 100% methanol and equilibrated with 2% acetonitrile (ACN) in 0.1% formic acid in LC-MS grade water. After loading, the C18 stage tips were washed with 2% ACN/0.1% formic acid and peptides separated from the HLA-I heavy chain and  $\beta$ 2-microglobulin species by eluting them with 50% ACN/0.1% formic acid. The ACN was evaporated by vacuum centrifugation and the peptides resuspended up to 6  $\mu$ l of volume in a solution of 2% ACN/0.1% formic acid and spiked with 10 fmol/ $\mu$ l of a cytomegalovirus pp65 495-503 peptide (NLVPMVATV) as internal control. For LC-MS analysis, 5  $\mu$ l of this peptide solution were used.

### ***LC-MS/MS***

Peptides were loaded and separated by a nanoflow HPLC (RSLC Ultimate 3000, Dionex) on a C18 Acclaim PepMap nanocolumn (50 cm length, 75  $\mu$ m internal diameter; Dionex) coupled on-line to a nano-electrospray ionization Q Exactive HF mass spectrometer (ThermoFisher) with a glass emitter (New Objective). Peptides were eluted with a linear gradient of 2–50% buffer B (80% ACN, 0.05% formic acid) at a flow rate of 220 nl/min over 60 min at 35°C. Data was acquired using a data-dependent acquisition “Top 20” method. We acquired one full-scan MS spectrum at a resolution of 60,000 at 200  $m/z$  with an automatic gain control (AGC) target value of  $3 \times 10^6$  ions, followed by 10 MS/MS spectra in higher energy collisional dissociation mode on the 10 most intense ions at a resolution of 15,000 at 200  $m/z$  with an AGC target value of  $1 \times 10^5$  with a maximum injection time of 120 ms and a dynamic exclusion of 20 s. Unassigned precursor ion charge states and charge states  $>4$  were excluded. The peptide match option was set to ‘preferred’. The resulting spectra were analyzed by MaxQuant ([www.coxdocs.org](http://www.coxdocs.org)) using a custom database comprising: *a*) the reference human proteome (Swiss-Prot/UniProt, up000005640, release December 2012); *b*) an in-house database containing 119,305 predicted peptide splice products (Berkers et al., 2015) from major known and candidate  $\beta$ -cell protein Ags (Fig. S1 and Data S1); and *c*) the predicted aa neo-sequences encoded by mRNA splice variants identified by RNASeq. The following parameters were set: enzyme specificity: unspecific; variable modifications: methionine, tryptophan and histidine oxidation (+15.99 Da), cysteine oxidation to cysteic acid (+47.98 Da) and tryptophan conversion to kynurenine (+3.99 Da); maximum false discovery rate 5%. Since the MS identification was targeted on HLA-I-eluted peptides rather than on proteins, the protein false discovery rate parameter was set to 100%. The initial allowed mass deviation of the precursor ion was set to 10 ppm and the maximum fragment mass deviation was set to 20 mDa. The “match between runs” option was enabled to match identifications across

different replicates in a time window of 0.5 min and an initial alignment time window of 20 min.

### ***RNAseq***

RNAs from 5 individual preparations of primary human islets exposed or not to IFN- $\gamma$  and IL-1 $\beta$  for 48 h and from HLA Class II<sup>lo</sup> and Class II<sup>hi</sup> human mTECs were sequenced on an Illumina HiSeq 2000 at high depth (coverage >150x10<sup>6</sup> reads, which is sufficient to detect >80% of splice variants). RNA sequencing reads were mapped to the human reference genome hg19 using TopHat 2 and the Gencode release 18 annotation dataset. Mapped reads were used to quantify abundance and analyse the differential expression of genes and transcripts using Flux Capacitor (Montgomery et al., 2010).

### ***HLA-I peptidomics and transcriptomics bio-informatics analysis***

Predicted HLA-I binding affinities for each nonamer peptide were visualized as sequence logo plots using Gibbs clustering ([www.cbs.dtu.dk/services/GibbsCluster](http://www.cbs.dtu.dk/services/GibbsCluster); Fig. 1D), and as heat maps (Fig. 1E) using the open-source script of Caron et al. (Caron et al., 2015).

For conventional peptides, source proteins were selected with Perseus ([www.coxdocs.org](http://www.coxdocs.org)) based on: *a*) a non-ubiquitous expression pattern, based on the Human Protein Atlas ([www.proteinatlas.org](http://www.proteinatlas.org)); *b*) a pancreas- and  $\beta$ -cell-enriched expression pattern, based on the Human Protein Atlas, the Human Protein Reference Database ([www.hprd.org](http://www.hprd.org)) and the Single-Cell Gene Expression Atlas of Human Pancreatic Islets (<http://sandberg.cmb.ki.se/pancreas>). The bioinformatics analysis pipeline is detailed in Fig. 1G. The 3,544 peptides identified were first filtered based on inter-sample reproducibility ( $\geq 2$  of 5 biological replicates; n=2,997, 85%) and aa length (8-12 aa; n=2,795, 93%). For all peptides, the final filter was based on an enrichment in HLA-I-purified samples compared with mock-purified ones based on *m/z* peak intensity, which verified the specific association of the identified peptides with pHLA-I complexes. From this dataset, we identified:

1) 217 (8%) peptides derived from ubiquitous proteins carrying PTMs (blue pipeline in Fig. 1G), from which 99 (46%; Table S2) were enriched in HLA-I-purified samples.

2) 15 (0.5%) peptide splice variants (brown pipeline in Fig. 1G; see Fig. S1 for the identification strategy), from which 10 (67%) were enriched in HLA-I-purified samples (listed in Table S1).

3) The remaining 2,561 peptides (both conventional and PTM species derived from  $\beta$ -cell-enriched proteins; red pipeline in Fig. 1G) were filtered by Perseus based on non-ubiquitous expression of their source proteins (n=411; 16%), using the Human Protein Atlas; and pancreas- and  $\beta$ -cell-enriched expression (n=139, 34%), using the Human Protein Atlas, the Human Protein Reference Database and the Single-Cell Gene Expression Atlas of Human Pancreatic Islets. Finally, the 86 (62%) remaining peptides were retained as enriched in HLA-I-purified samples (listed in Table S1).

4) mRNA splice variants (green pipeline in Fig. 1G; n=2, 0.1%; both enriched in HLA-purified samples; listed in Table S1) were identified by analyzing the HLA-I peptidomics dataset against the predicted aa neo-sequences obtained from RNAseq analysis. For this RNAseq pipeline (dashed boxes in Fig. 1G), 53,280 mRNAs were filtered based on:

a) A median RPKM > 5 in islets, either under basal or inflammatory conditions, a cut-off selected based on the median RPKM of known islet Ags (islet expression filter; n=14,504, 27%).

b) A median RPKM < 0.1 in mTECs (either HLA Class II<sup>lo</sup> or Class II<sup>hi</sup>), or a median RPKM fold-decrease > 100 vs. islet (mTEC expression filter; n=908, 6%).

c) A median RPKM fold-increase > 10 in islets compared to 12 control tissues (adipose tissue, breast, colon, heart, kidney, liver, lung, lymph node, ovary, prostate, skeletal muscle, white blood cells), using the Illumina BodyMap 2.0 dataset (islet enrichment filter; n=166, 18%).

Tissues of neuroendocrine origin (brain, testis, adrenal gland and thyroid) were excluded for this filtering.

d) We subsequently focused our analysis on mRNA isoforms, as described (Eizirik et al., 2012; Villate et al., 2014). The predicted translation products were aligned using MUSCLE 3.8 ([www.ebi.ac.uk/Tools/msa/muscle](http://www.ebi.ac.uk/Tools/msa/muscle)), and aa neo-sequences were defined by comparing the predicted aa sequence of each mRNA isoform with that of the reference mRNA, taking as reference the longest and/or most prevalent mRNA isoform in islets (neo-sequence generation filter; n=88, 53%).

The 336 predicted aa neo-sequences obtained from these 88 mRNA variants were used to interrogate HLA-I peptidomics datasets and searched in parallel for:

e) Potential HLA-A2 binders, based on their predicted HLA-A2 binding affinity ( $K_D < 100$  nM by NetMHC 4.0; [www.cbs.dtu.dk/services/NetMHC](http://www.cbs.dtu.dk/services/NetMHC)) and stability (half-life  $\geq 1.5$  h by NetMHCstab 1.0; [www.cbs.dtu.dk/services/NetMHCstab-1.0](http://www.cbs.dtu.dk/services/NetMHCstab-1.0)) (predicted HLA-A2 binding filter; n=66, 20%).

f) A 9-10-aa length (peptide length filter; n=43, 65%).

g) A neo-sequence  $\geq 3$  aa (neo-sequence filter; n=39, 92%).

Overall, this combined HLA-I peptidomics and transcriptomics analysis pipeline led to the identification of 99 *in vitro* PTM candidates from ubiquitous proteins (Table S2); 10 *in vitro* peptide splice candidates, 86 *in vitro* candidates from  $\beta$ -cell proteins (including PTM variants) and 2 *in vitro* mRNA splice candidates (Table S1); and 39 *in silico* mRNA splice candidates (Fig. S2I). PTM candidates were not further analyzed. The other candidates underwent additional filtering steps to focus subsequent studies on HLA-A2-restricted peptides. Predicted HLA-A2 binders were first selected *in silico* using NetMHC 4.0 and NetMHCstab 1.0 (except for *in silico* mRNA splice candidates, which had already been filtered for

predicted HLA-A2 binding in the same way), then *in vitro* for experimental HLA-A2 binding and, finally, for CD8<sup>+</sup> T-cell recognition.

### ***HLA-A2 binding assays***

Peptide binding to HLA-A\*02:01 was measured using the transporter associated with Ag processing (TAP)-deficient T2 cell line. TAP deficiency leads to defective translocation of endogenous peptides from the cytosol into the ER, leading to the expression of unstable, empty HLA-A\*02:01 molecules on the cell surface. This expression is stabilized in the presence of HLA-A\*02:01-binding peptides, resulting in a higher surface expression that can be monitored by flow cytometry. T2 cells were washed in RPMI medium and plated in round-bottom 96-well plates at  $0.2 \times 10^6$  cells/200  $\mu$ l in the presence of 5  $\mu$ g/ml  $\beta$ 2-microglobulin. Peptides prepared in DMSO were sequentially diluted 4-fold in RPMI and added to final concentrations of 102.4 to 0.1  $\mu$ M for 24 h at 37°C, 5% CO<sub>2</sub>. The HLA-A\*02:01-binding peptide Flu MP<sub>58-66</sub> (GILGFVFTL), and a non-binding peptide CHGA<sub>382-390</sub> (HPVGEADYF) were included as positive and negative controls, respectively. After incubation, the cells were washed twice with ice-cold phosphate-buffered saline (PBS) and stained with the viability marker Live/Dead Red and mouse anti-HLA-A2 mAb BB7.2, followed by an Alexa Fluor 488-labeled goat-anti-mouse IgG Ab (Interchim). Following acquisition on a BD Fortessa cytometer, results were analyzed by gating on viable cells and expressed as the median fluorescence intensity fold increase of the test peptide compared with the negative control peptide at the same concentration.

### ***HLA-A2 MMr assays***

All peptides were synthesized at >90% purity (Synpeptides). HLA-A2 MMrs were produced and used as described (Culina et al., 2018). Each pHLA-A2 complex was used at a final concentration of 8-27 nM and conjugated with fluorochrome-labeled streptavidin at a 1:4 ratio. The combinatorial MMr panel was first set up by staining HLA-A2<sup>+</sup> PBMCs with the



same set of fluorescent streptavidin-labeled MMrs, all loaded with the Flu MP<sub>58-66</sub> epitope. Compensations were set using fluorescence-minus-one samples (i.e. omitting one streptavidin at a time). The concentration of each fluorescent MMr was corrected for the variable staining index of each streptavidin, in order to obtain a distinct double-MMr<sup>+</sup> population for each fluorochrome pair. The identification of the same MMr<sup>+</sup> population by each pair validated the panel. PBMCs were isolated by density gradient centrifugation using 50 ml Leucosep® tubes (Greiner/Dominique Dutscher), washed twice in RPMI medium supplemented with AB human serum (Sigma), counted on a ThermoFisher Countess II automated counter and frozen in pre-chilled 10% DMSO solution in AIM-V medium (ThermoFisher) using CoolCell containers (Biocision) stored overnight at -80°C prior to transfer into liquid nitrogen. At thawing, PBMCs were immediately diluted in pre-warmed AIM-V medium. Following centrifugation and one additional wash in AIM-V, PBMCs were counted and rested in the presence of 50 nM dasatinib for 30 min at 37°C before magnetic depletion of CD8<sup>-</sup> cells (StemCell Technologies). Staining was performed for 20 min at 20°C in 20 µl PBS-dasatinib for 10<sup>7</sup> cells with the combinatorial double-coded MMr panels (Culina et al., 2018) detailed in Fig. 3, followed, without washing, by mAb and Live/Dead Aqua staining at 4°C for 20 min. After one wash, cells were acquired using a FACS Aria III cytometer configured as detailed in Table S6. Candidate epitopes binding to HLA-A2 (Fig. S2) that did not yield any appreciable MMr staining provided negative controls for each panel. Data was analyzed with FlowJo software as described in Fig. 3. Cells were sequentially gated on small lymphocytes, singlets, live cells (Live/Dead Aqua<sup>-</sup>), CD3<sup>+</sup>CD8<sup>+</sup> T cells and total PE<sup>+</sup>, PE-CF594<sup>+</sup>, APC<sup>+</sup>, BV650<sup>+</sup>, BV711<sup>+</sup> and BV786<sup>+</sup> MMr<sup>+</sup> T cells. Using Boolean operators, these latter gates allowed to selectively visualize each double-MMr<sup>+</sup> population by including only those events positive for the corresponding fluorochrome pair. For example, UCN3<sub>1-9</sub> MMr<sup>+</sup> cells (PE<sup>+</sup>PE-CF594<sup>+</sup>) were visualized by gating on events that were PE<sup>+</sup>PE-CF594<sup>+</sup>APC<sup>-</sup>BV650<sup>-</sup>BV711<sup>-</sup>BV786<sup>-</sup>.

Events negative for all MMr fluorochromes (PE<sup>-</sup>PE-CF594<sup>-</sup>APC<sup>-</sup>BV650<sup>-</sup>BV711<sup>-</sup>BV786<sup>-</sup>) were represented in the same PE/PE-CF-594 dot plot to set the double-MMr<sup>+</sup> gate, as shown in Fig. 4A-F. CD45RA and CCR7 staining was subsequently visualized by gating on these MMr<sup>+</sup> cells. Each dot plot of Fig. 3B-C displays a color-coded overlay of each double-MMr<sup>+</sup> fraction and of the MMr<sup>-</sup> population to visualize the separation of each epitope-reactive CD8<sup>+</sup> T-cell fraction relative to the others.

### ***In-situ HLA-A2 MMr staining***

*In-situ* immunohistochemistry staining was performed as described (Culina et al., 2018). Unfixed, frozen sections were dried for 2 h, loaded with 1 µg of PE-labeled MMrs overnight at 4°C, washed gently with PBS and fixed in 2% paraformaldehyde for 10 min. After a further wash, endogenous peroxidase activity was blocked with 0.3% H<sub>2</sub>O<sub>2</sub>. Sections were then incubated serially with a rabbit anti-PE Ab (Abcam), horseradish peroxidase-conjugated swine anti-rabbit Ig (Dako) and 3,3'-diaminobenzidine tetrahydrochloride substrate (ThermoFisher). After a final wash, sections were counterstained with hematoxylin, dehydrated via sequential passages in 95-100% ethanol and xylene, mounted and analyzed using a Nikon Eclipse Ni microscope with NIS-Elements D software v4.40.

*In-situ* immunofluorescence staining was performed similarly, but non-specific reactions were blocked with 5% goat serum for 2 h at room temperature before serial incubations with rabbit anti-PE Ab (1:250, 1.5 h at room temperature) and Alexa Fluor 594-conjugated goat anti-rabbit IgG (ThermoFisher; 1:500, 1 h at room temperature). After a further wash, sections were incubated for 1 h at room temperature with rat anti-CD8 mAb (Abcam; 1:100) together with mouse anti-CD45RO mAb (BioLegend; 1:200) followed, after one wash, by one final incubation for 1 h at room temperature with Alexa Fluor 488-conjugated goat anti-rat IgG together with Alexa Fluor 647-conjugated goat anti-mouse IgG (1:500/each; both from

ThermoFisher). After DNA counterstaining with DAPI, sections were mounted and analyzed using a Leica TCS SP5 confocal laser scanning microscope with LAS software v2.6.0.7266.

### **Quantification and statistical analysis**

Statistical details of experiments can be found in the legends of each figure. A two-tailed  $p < 0.05$  cut-off was used to define statistical significance.

### **Data and software availability**

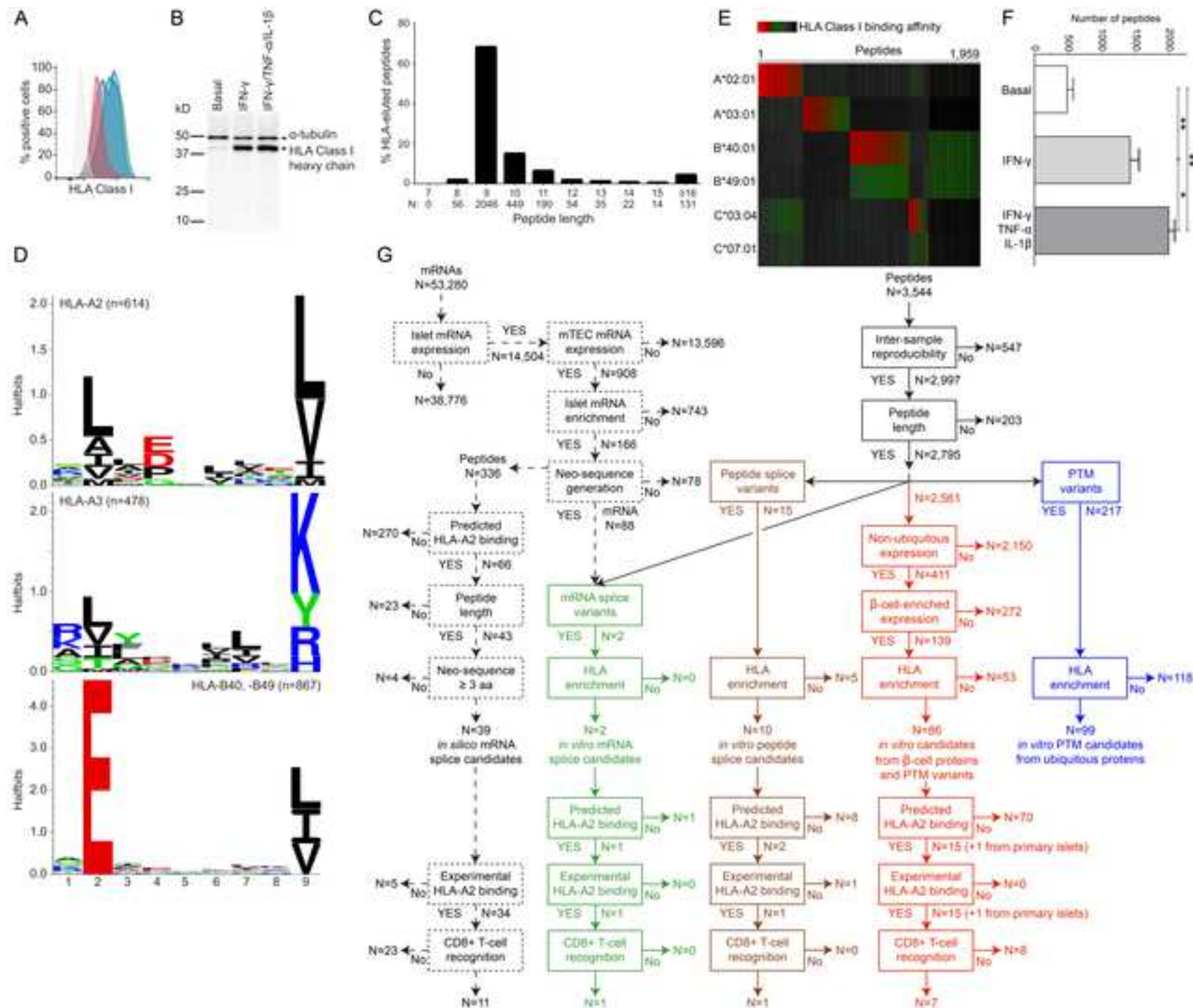
The custom script used to predict peptide splice products is provided in Data S1. The islet RNAseq datasets have been deposited under GEO accession number GSE108413. The mTEC RNAseq dataset is provided in Data S2.

## **SUPPLEMENTAL DATA**

**Data S1.** Related to Fig. 1G-S1. In-house script used to predict peptide splice products.

**Data S2.** Related to Fig. 1G. mTEC RNAseq dataset of mRNA isoforms expressed in human islets.

Figure 1

[Click here to download Figure Fig1.tif](#)


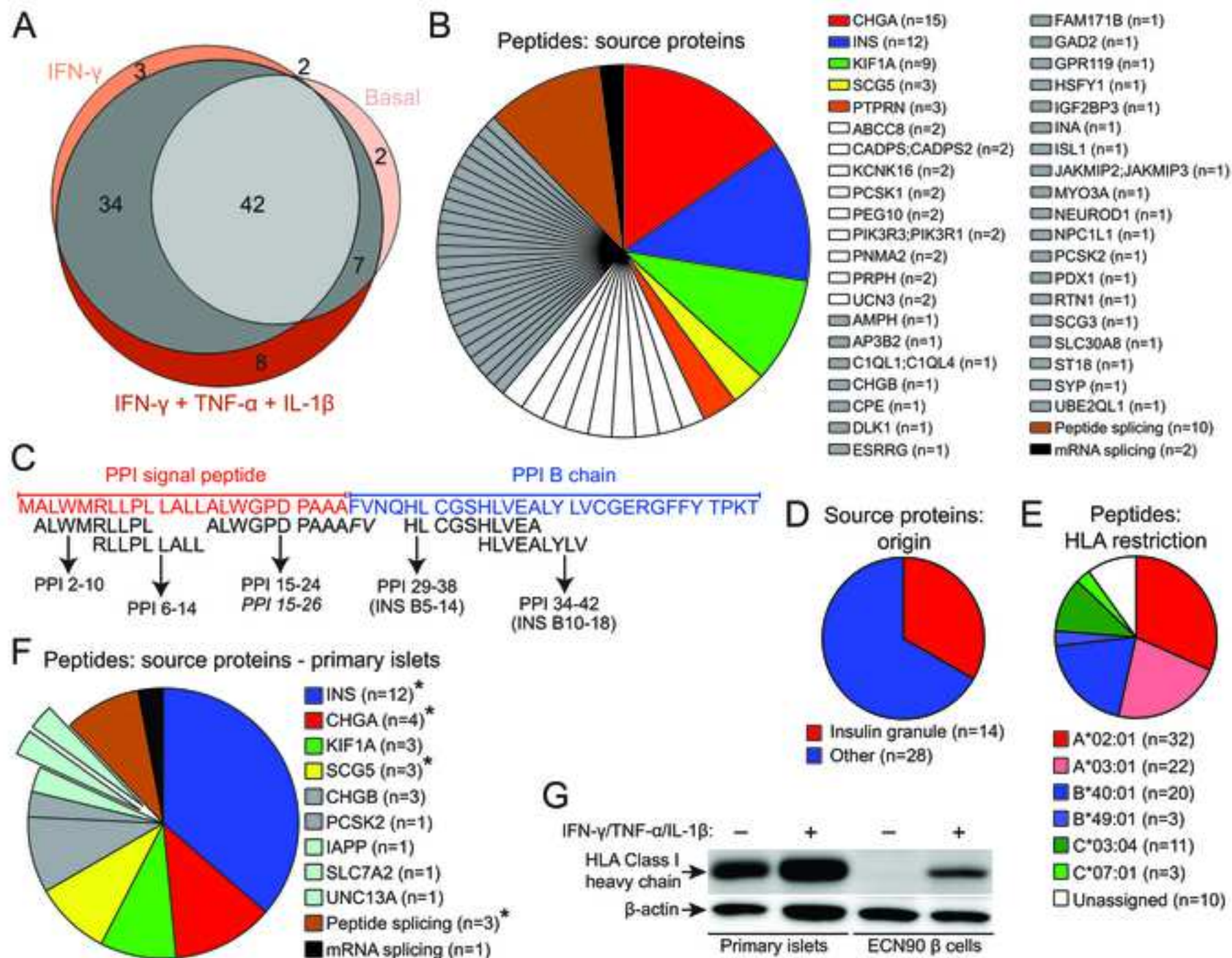




Figure 3

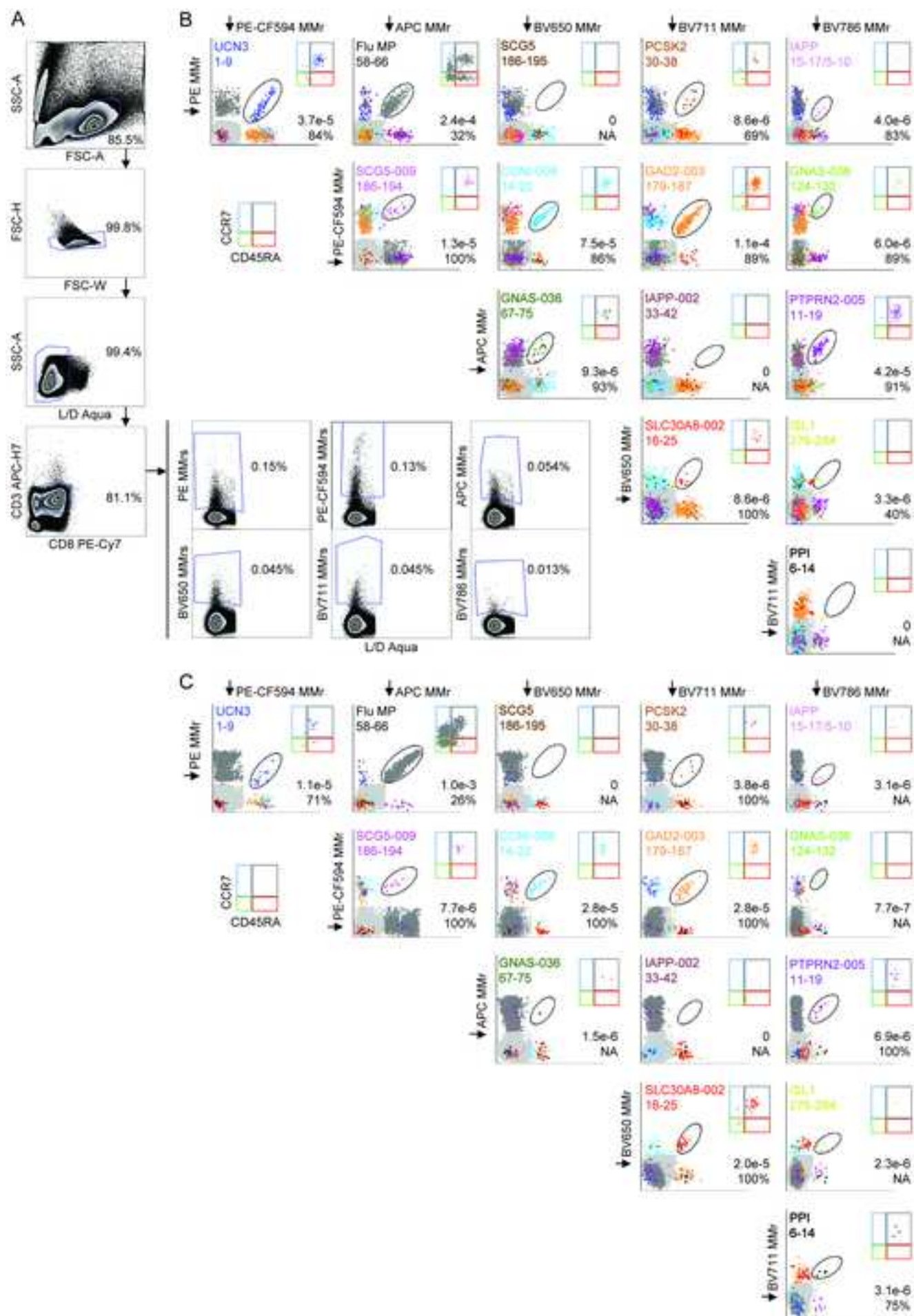
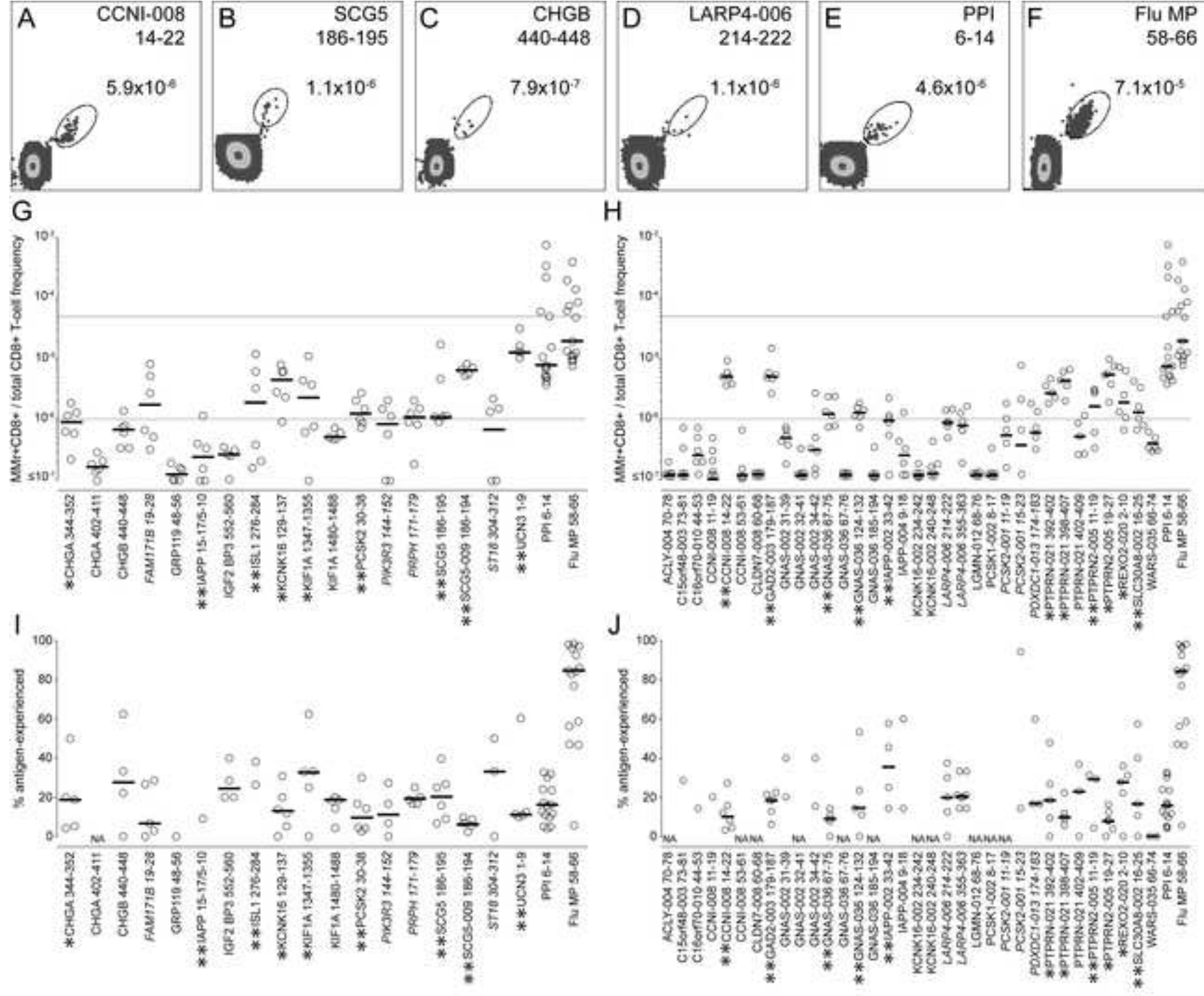
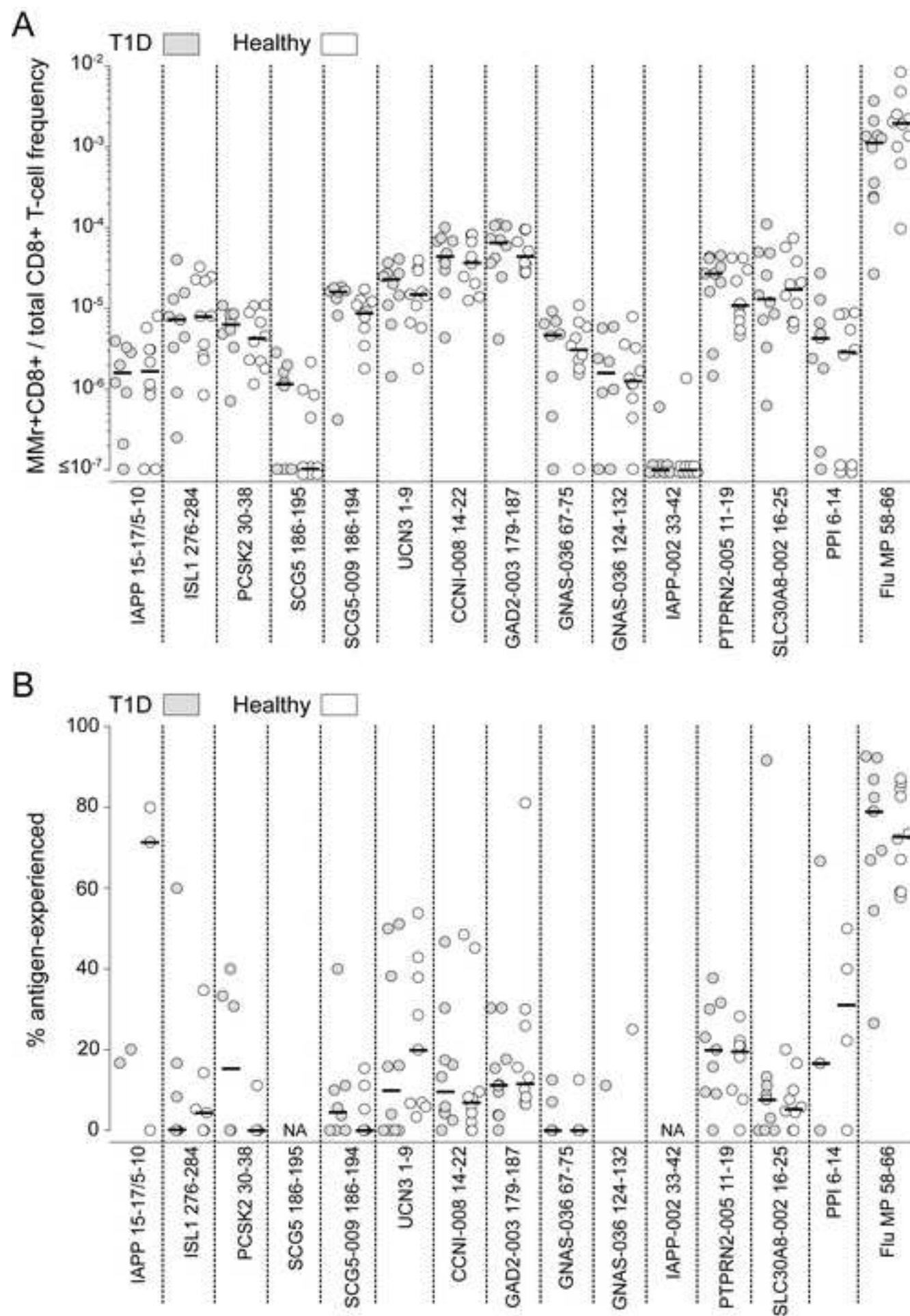
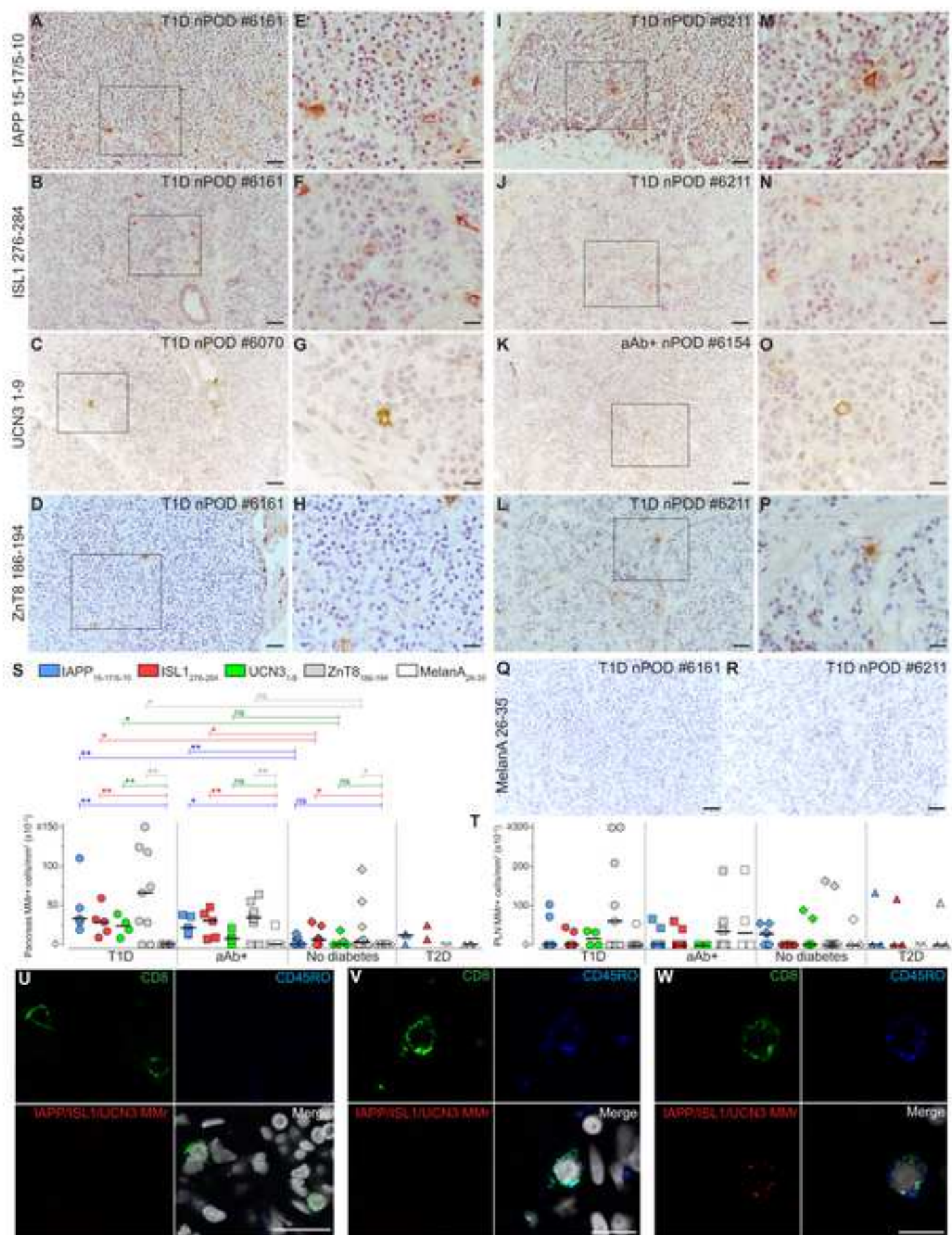
[Click here to download Figure Fig3.tif](#)

Figure 4

[Click here to download Figure Fig4.tif](#)









## KEY RESOURCES TABLE

REAGENT or RESOURCE	SOURCE	IDENTIFIER
Antibodies		
Mouse monoclonal anti-HLA Class I, clone W6/32	ATCC	ATCC HB-95; RRID: CVCL_7872
Mouse monoclonal anti-HLA Class I, clone HC10	Laboratory of Hidde L. Ploegh	RRID: AB_2728622
Mouse monoclonal anti- $\alpha$ -tubulin, clone DM1A	Thermo Fisher eBioscience	Cat#14-4502-80; RRID: AB_1210457
Mouse monoclonal anti- $\beta$ -actin, clone AC-15	Sigma	Cat#A5441; RRID: AB_476744
Goat polyclonal Anti-mouse Ig (H+L) HRP	SouthernBiotech	Cat#1010-05; RRID: AB_2728714
Mouse monoclonal anti-HLA-A2, clone BB7.2	ATCC	ATCC HB-82; RRID: CVCL_7246
Goat polyclonal anti-mouse Ig FITC	BD Pharmingen	Cat#554001; RRID: AB_395197
Goat polyclonal anti-mouse IgG (H+L) Alexa Fluor 488	Interchim	Cat#FP-SA4010; RRID: AB_2728715
EasySep™ Human CD8+ T Cell Enrichment Kit	StemCell Technologies	Cat#19053; RRID: AB_2728716
Mouse monoclonal anti-human CD3 APC-H7, clone SK7	BD Pharmingen	Cat#560176; RRID: AB_1645475
Mouse monoclonal anti-human CD8 PE-Cy7, clone RPA-T8	BD Pharmingen	Cat#557746; RRID: AB_396852
Mouse monoclonal anti-human CD45RA FITC, clone HI100	BD Pharmingen	Cat#555488; RRID: AB_395879
Mouse monoclonal anti-human CCR7 BV421, clone 150503	BD Horizon	Cat#562555; RRID: AB_2728119
LIVE/DEAD™ Fixable Aqua Dead Cell Stain Kit	Thermo Fisher	Cat#L34965
LIVE/DEAD™ Fixable Red Dead Cell Stain Kit	Thermo Fisher	Cat# L23102
Streptavidin PE	BD Pharmingen	Cat#554061; RRID: AB_10053328
Streptavidin PE-CF594	BD Horizon	Cat#562284; RRID: AB_11154598
Streptavidin APC	BD Pharmingen	Cat#554067; RRID: AB_10050396
Streptavidin BV650	BD Horizon	Cat#563855
Streptavidin BV711	BD Horizon	Cat#563262
Streptavidin BV786	BD Horizon	Cat#563858
Rabbit polyclonal anti-B phycoerythrin	Abcam	Cat#ab7011; RRID: AB_305700
Swine polyclonal anti-rabbit Ig HRP	Dako	Cat#P0217; RRID: AB_2728719
Rat monoclonal anti-human CD8, clone YTC182.20	Abcam	Cat#ab60076; RRID: AB_940921
Mouse monoclonal anti-human CD45RO, clone UCHL1	BioLegend	Cat#304202; RRID: AB_314418
Goat polyclonal anti-rabbit IgG (H+L) Alexa Fluor 594	Thermo Fisher	Cat#A-11037; RRID: AB_2534095
Goat polyclonal anti-rat IgG (H+L) Alexa Fluor 488	Thermo Fisher	Cat# A-11006; RRID: AB_2534074

Goat polyclonal anti-mouse IgG (H+L) Alexa Fluor 647	Thermo Fisher	Cat# A-21236; RRID: AB_2535805
Bacterial and Virus Strains		
Biological Samples		
Human pancreas unfixed frozen sections	nPOD	www.jdrfnpod.org
Human pancreatic lymph node unfixed frozen sections	nPOD	www.jdrfnpod.org
Chemicals, Peptides, and Recombinant Proteins		
HLA-A2 heavy chain	ImmunAware	N/A
$\beta$ 2-microglobulin	Lee Biosolutions	Cat#126-11
Dasatinib	LC Laboratories	Cat#D-3307
Critical Commercial Assays		
Deposited Data		
Human reference proteome Swiss-Prot/UniProt, up000005640, release December 2012	Uniprot	http://www.uniprot.org/proteomes/UP000005640
Human Protein Atlas v.13.0	Human Protein Atlas	www.proteinatlas.org
Human Protein Reference Database, release 9	Human Protein Reference Database	www.hprd.org
Single-Cell Gene Expression Atlas of Human Pancreatic Islets	Sandberg Lab	http://sandberg.cmb.ki.se/pancreas
Gencode release 18	The GENCODE Project	https://www.gencodegenes.org
Illumina BodyMap 2.0	http://www.ncbi.nlm.nih.gov/sra/?term=E-MTAB-513	GEO #GSE30611
Human islet RNAseq	This paper	GEO # GSE108413
Human mTEC RNAseq	This paper	Data S2
Experimental Models: Cell Lines		
Human: ECN90 $\beta$ -cell line	Culina et al., 2018; Univercell Biosolutions	N/A
Human: T2 (174 x CEM.T2) cell line	ATCC	ATCC CRL-1992; RRID: CVCL_2211
Mouse: W6/32 hybridoma cell line	ATCC	ATCC HB-95; RRID: CVCL_7872
Mouse: HC10 hybridoma cell line	Laboratory of Hidde L. Ploegh	RRID: AB_2728622
Mouse: BB7.2 hybridoma cell line	ATCC	ATCC HB-82; RRID: CVCL_7246
Experimental Models: Organisms/Strains		
Oligonucleotides		
Recombinant DNA		
Software and Algorithms		
FlowJo v10	FlowJo, LLC	www.flowjo.com

Flux Capacitor v1.6.1	Montgomery et al., 2010	<a href="http://sammeth.net/confluence/display/FLUX/Home">http://sammeth.net/confluence/display/FLUX/Home</a>
Gibbs clustering v1.1	DTU Bioinformatics	<a href="http://www.cbs.dtu.dk/services/GibbsCluster">www.cbs.dtu.dk/services/GibbsCluster</a>
LAS v2.6.0.7266	Leica Microsystems	N/A
MaxQuant v1.5.3.8	Max Planck Institute of Biochemistry	<a href="http://www.coxdocs.org">http://www.coxdocs.org</a>
MUSCLE v3.8	EMBL-EBI	<a href="http://www.ebi.ac.uk/Tools/msa/muscle">www.ebi.ac.uk/Tools/msa/muscle</a>
NetMHC v4.0	DTU Bioinformatics	<a href="http://www.cbs.dtu.dk/services/NetMHC">www.cbs.dtu.dk/services/NetMHC</a>
NetMHCstab v1.0	DTU Bioinformatics	<a href="http://www.cbs.dtu.dk/services/NetMHCstab-1.0">www.cbs.dtu.dk/services/NetMHCstab-1.0</a>
NetMHCStabPan v1.0	DTU Bioinformatics	<a href="http://www.cbs.dtu.dk/services/NetMHCstabpan">www.cbs.dtu.dk/services/NetMHCstabpan</a>
NIS-Elements D v4.40	Nikon	N/A
Perseus v1.5.2.4	Max Planck Institute of Biochemistry	<a href="http://www.coxdocs.org">http://www.coxdocs.org</a>
Python and R Scripts	Caron et al., 2015	<a href="https://elifesciences.org/articles/07661/figures#SD9-data">https://elifesciences.org/articles/07661/figures#SD9-data</a>
Script for the prediction of peptide splice products	This paper	Data S1
TopHat v2.0.10	J. Hopkins University Center for Computational Biology	<a href="http://ccb.jhu.edu/software/tophat/index.shtml">http://ccb.jhu.edu/software/tophat/index.shtml</a>
Other		

## SUPPLEMENTAL ITEMS

**Figure S1.** Related to Fig. 1G. Schematic of the strategy used for predicting peptide splice variants.

**Figure S2.** Related to Fig. 4. HLA-A2 binding measurements for the  $\beta$ -cell peptides selected for CD8<sup>+</sup> T-cell validation.

**Fig. S3.** Related to Fig. 6. Screening of HLA-A2-restricted peptide reactivities in pancreas-infiltrating cells from a T1D case.

**Table S1. Related to Fig 1G, 2A-E. List of the 98 HLA-I-bound peptides identified in ECN90  $\beta$  cells.**

**Table S2.** Related to Fig 1G. List of the 99 HLA-I-bound PTM peptides originating from ubiquitous proteins identified in ECN90  $\beta$  cells.

**Table S3.** Related to Fig 2F. List of the 33 HLA-I-bound peptides identified in primary human islets.

**Table S4.** Related to Fig. 4-5. Characteristics of HLA-A2<sup>+</sup> study subjects for ex-vivo MMr studies on PBMCs.

**Table S5.** Related to Fig. 6. nPOD cases analyzed by *in-situ* tissue MMr staining.

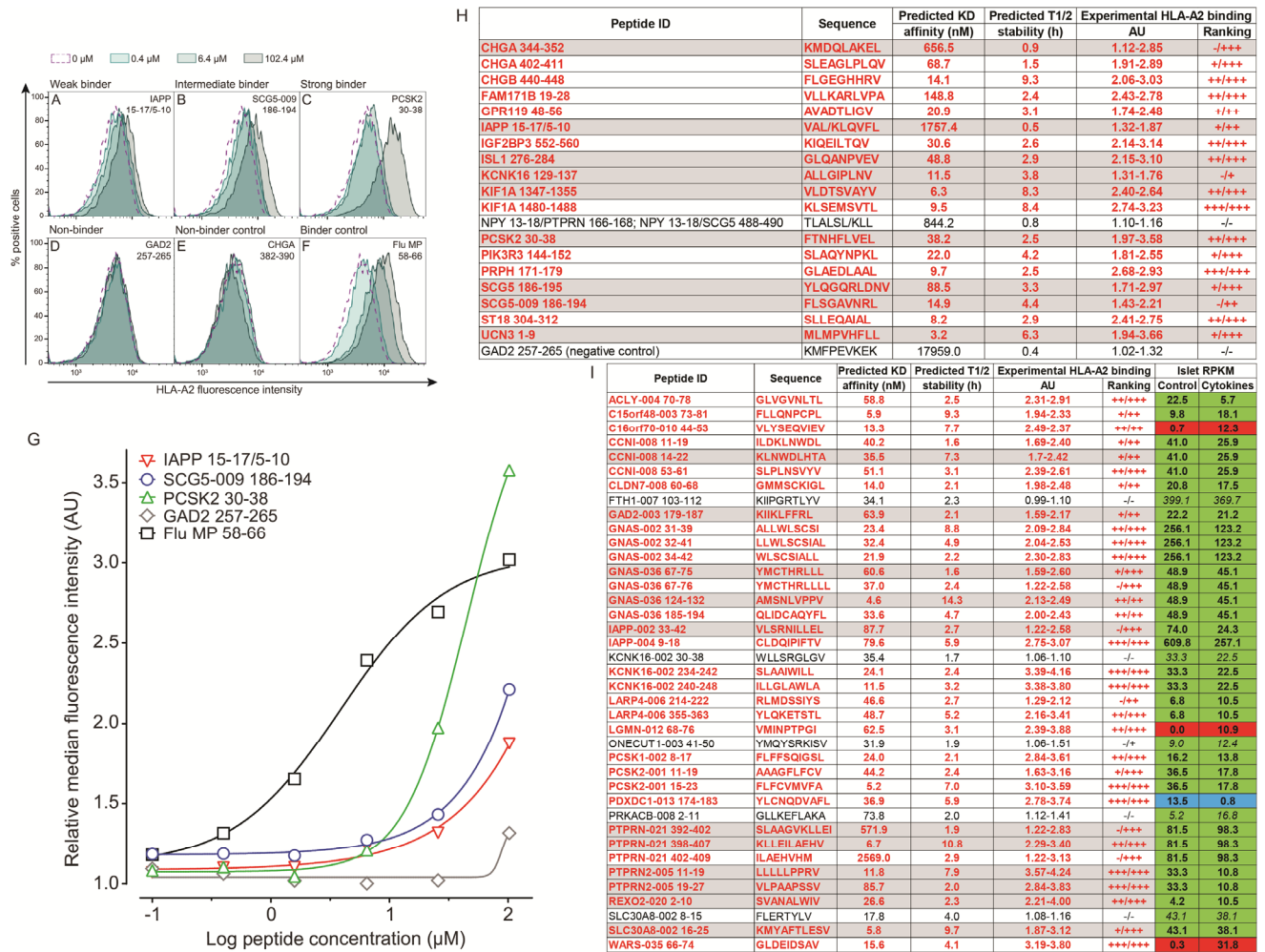
**Table S6.** Related to STAR Methods. Configuration of the flow cytometer used for HLA-A2 MMr assays.

**Data S1.** Related to Fig. 1G-S1. In-house script used to predict peptide splice products.

**Data S2.** Related to Fig. 1G. mTEC RNAseq dataset of mRNA isoforms expressed in human islets.

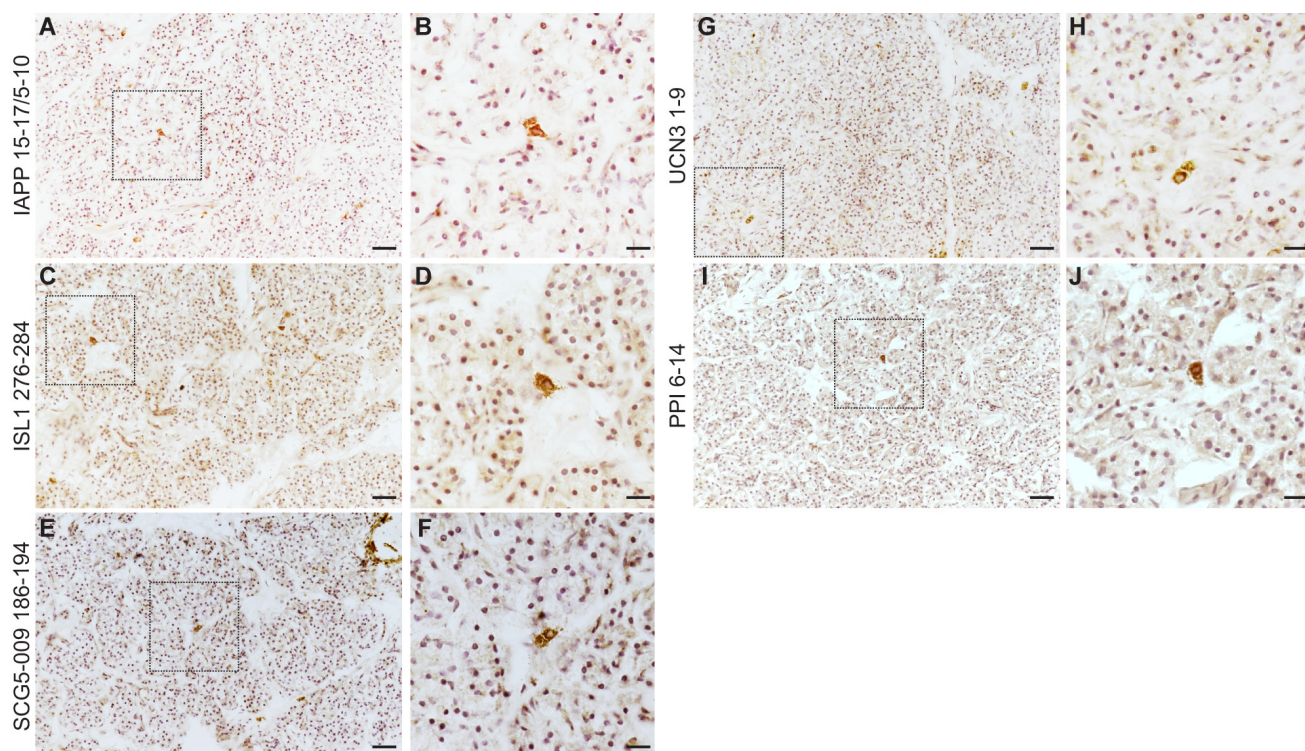
Source protein	N-terminal precursor sequence	C-terminal precursor sequence	N-terminal precursor	C-terminal precursor	Cis splice peptide candidates	Trans splice peptide candidates
PPI	P1: D/E/Q/N/S/T/Φ P2: G/A/N/Q/S/T/D/E/Φ P3-P9: any	P1': K/R P2': Φ P3': Φ P4'-P9': any	PPI-1	PPI-A	PPI-1 / PPI-A	PPI-1 / IGRP-A
			PPI-2		PPI-2 / PPI-A	PPI-1 / IGRP-B
IGRP			IGRP-1	IGRP-A	IGRP-1 / IGRP-A	PPI-2 / IGRP-A
				IGRP-B	IGRP-1 / IGRP-B	PPI-2 / IGRP-B
						IGRP-1 / PPI-A
CHGA						...
SCG5						
PTPRN						
NPY						
SLC30A8						
IAPP						
PCSK2						
GAD2						

**Figure S1. Related to Fig. 1G. Schematic of the strategy used for predicting peptide splice variants.** The indicated known or putative β-cell Ags (first column; PPI, IGRP, CHGA, SCG5, PTPRN/IA-2, NPY, SLC30A8/ZnT8, IAPP, PCSK2, GAD2/GAD65) were scanned with an in-house Python script (Data S1) based on reported peptide splicing preferences (Berkers et al., 2015) for the presence of the indicated N- and C-terminal preferred precursor sequences (second and third column, respectively, where Φ indicates any hydrophobic aa residue). Each N-terminal precursor sequence identified was then combined with each C-terminal precursor sequence, derived either from the same protein (*cis*-splicing) or from a different protein (*trans*-splicing). An example is shown for PPI and IGRP. The 119,305 predicted peptide splice sequences thus obtained (26,396 *cis*-spliced and 92,909 *trans*-spliced) were saved in FASTA format and appended to the Swiss-Prot human proteome database used for assigning aa sequences to the identified MS spectra with the MaxQuant algorithm.



**Figure S2. Related to Fig. 4. HLA-A2 binding measurements for the  $\beta$ -cell peptides selected for CD8<sup>+</sup> T-cell validation. (A-F)** Flow cytometry measurement of peptide binding to HLA-A2 using TAP-deficient T2 cells. T2 cells were pulsed with the indicated peptides at 4-fold sequential dilutions (102.4 to 0.1  $\mu$ M) at 37°C and stained for HLA-A2. Representative stains at 0.4, 6.4 and 102.4  $\mu$ M are shown for peptides that are weak binders (IAPP<sub>15-17/5-10</sub>; A), intermediate binders (SCG5-009<sub>186-194</sub>; B), strong binders (PCSK2<sub>30-38</sub>; C) and non-binders (GAD2<sub>257-265</sub>; D), along with the non-binding (ChgA<sub>382-390</sub>; E) and binding (Flu MP<sub>58-66</sub>; F) control peptides included in each assay. **G.** Plotting of relative median fluorescence intensity values (arbitrary units, AU) for all peptide dilutions normalized to the non-binding ChgA<sub>382-390</sub> control peptide. Representative examples of two independent experiments are shown. **(H-I)** Summary of the HLA-A2 binding values measured for the  $\beta$ -cell peptides selected from the *in vitro* HLA-I peptidomics (H) and *in silico* RNAseq pipeline (I) using the T2 assays depicted in panels A-G. The relative median fluorescence intensity measured at 25.6 and 102.4  $\mu$ M peptide concentrations is shown along with their relative ranking: – (<1.50 AU); + (1.50-1.99 AU); ++ (2-2.49 AU); +++ ( $\geq$ 2.50 AU). The *in silico* predicted HLA-A2 binding affinity (NetMHC 4.0) and stability values (NetMHCstab 1.0) are also shown. Peptides in bold red fonts bound HLA-A2 and were retained for CD8<sup>+</sup> T-cell validation, with those eventually validated (see Fig. 4) highlighted in grey. In panel H, the GAD2<sub>257-265</sub> peptide eluted from ECN90 cells with a predicted HLA-A3 restriction is included as negative control. For  $\beta$ -cell peptides selected from the *in silico* RNAseq pipeline (panel I), RPKM values of the source mRNA splice variant in control- and cytokine-treated islets are shown in the last two columns. The color codes indicate no change in mRNA expression (<2 log<sub>2</sub> fold-change, either positive or negative; green), an increase for cytokine-treated islets ( $\geq$ +2 log<sub>2</sub> fold-change; red) or a decrease for cytokine-treated islets ( $\leq$ -2 log<sub>2</sub> fold-change; blue).





**Fig. S3. Related to Fig. 6. Screening of HLA-A2-restricted peptide reactivities in pancreas-infiltrating cells from a T1D case.** Pancreas sections from T1D EUnPOD case #060217 (39-year-old female, T1D duration 21 years, positive for anti-GAD aAbs) were immunohistochemically stained *in situ* with the following MMRs: IAPP<sub>15-17/5-10</sub> (A-B), ISL1<sub>276-284</sub> (C-D), SCG5-009<sub>186-194</sub> (E-F), UCN3<sub>1-9</sub> (G-H) and the positive control PPI<sub>6-14</sub> (I-J). For each MMR, pancreas images at 20X magnification are shown on the left (scale bar 100  $\mu$ m), and higher magnifications of the dotted areas are shown on the right (scale bar 36  $\mu$ m).





Source protein(s)	Accession number(s)	Aminoacid positions	Sequence	HLA restriction	Predicted affinity (nM)	Predicted stability (h)	IFN- $\gamma$ /TNF- $\alpha$ /IL-1 $\beta$ log2 FC
INS (n=12)	P01308	2-10	ALWMRLPL	A*02:01	26.7	5.6	Basal only
		2-12*	ALWMRLPLLA	A*02:01	83.8	2.8	-2.16
		5-13	MRLLPLAL	B*39:01	71.4	0.6	1.71
		5-13	M(+16)RLPLAL	B*39:01	71.4	0.6	Basal only
		15-24	ALWGPDPA	A*02:01	95.5	1.8	-3.26
		15-24	ALW(+16)GPDPA	A*02:01	95.5	1.8	-3.58
		15-24	ALW(+4)GPDPA	A*02:01	95.5	1.8	Basal only
		17-24*	WGPDPA	NA	NA	NA	-3.87
		29-38	HLCGSHLVEA	A*02:01	521.1	1.5	6.64
		33-41	SHLVEALYL	B*39:01	283.8	0.4	IFN- $\gamma$ /TNF- $\alpha$ /IL-1 $\beta$ only
		34-42	HLVEALYLV	A*02:01	3.3	17.8	Basal only
		57-67*	EAEDLQVGQVE	NA	NA	NA	0.13
CHGA (n=4)	P10645	344-352	KMDQLAKEL	A*02:01	543.8	0.6	0.04
		344-354	KMDQLAKELTA	A*02:01	823.2	0.6	-1.68
		381-390	YGFRGPGPQL	C*12:03, C*14:02	150.2, 139.9	0.2, 0.2	-0.37
		383-390	FRGPGPQL	B*39:01	380.7	0.7	-0.90
KIF1A (n=3)	Q12756	791-800	DQKNGATHYW	NA	NA	NA	-1.08
		1058-1066	EVTKSFIIEY	A*25:01	370.6	1.3	-1.86
		1319-1327	NRVTGVYEL	B*39:01	19.8	0.7	-0.72
SCG5 (n=3)	P05408	136-144	DTAEFSREF	A*25:01	187.4	0.7	4.61
		186-195*	YLQGQRLDNV	A*02:01	44.8	2.2	1.77
		186-196	YLQGQRLDNVV	A*02:01	151.8	1.7	-1.19
CHGB (n=3)	P05060	429-437	YFMSDTREE	C*14:02	1857.7	0.1	Basal only
		429-437	YFM(+16)SDTREE	C*14:02	1857.7	0.1	IFN- $\gamma$ /TNF- $\alpha$ /IL-1 $\beta$ only
		440-448	FLGEGHHRV	A*02:01	4.4	8.6	-3.35
PCSK2 (n=1)	P16519	26-34	ERPVTNHF	C*14:02	3731.5	0.1	0.74
IAPP (n=1)	P10997	23-30	TPIESHQV	B*51:01	1423.2	1.1	1.84
SLC7A2 (n=1)	P52569	650-658	IFHEKTSEF	C*14:02	27.4	0.3	0.33
UNC13A (n=1)	Q9UPW8	1234-1243	DIISKDFASY	A*25:01	73.9	0.8	-0.58
IAPP/IAPP;PTPRN/IAPP	P10997/P10997;Q16849/P10997	15-17/5-10;596-598/5-10	VAL/KLQVFL	A*02:01, C*12:03	3599.1, 3763.0	0.5, 0.1	-0.58
SCG5/PCSK2;SLC30A8/PCSK2	P05408/P16519;Q8IWU4/P16519	113-115/565-570;168-170/565-570	YPD/RGTWTL	B*39:01	10.0	0.8	IFN- $\gamma$ /TNF- $\alpha$ /IL-1 $\beta$ only
PTPRN/IAPP	Q16849/P10997	795-802/44-48	WQM(+16)VWESG/RLANF	B*39:01, C*14:02	1487.1, 1801.9	0.3, 0.2	1.84
WARS-035	WARS-035	18-26	SVAQAGVHW	NA	NA	NA	IFN- $\gamma$ /TNF- $\alpha$ /IL-1 $\beta$ only

**Table S3. Related to Fig 2F. List of the 33 HLA-I-bound peptides identified in primary human islets.** The same bioinformatics filters used for ECN90  $\beta$  cells (Fig. 1G) were applied, barring the inter-sample reproducibility and HLA-I enrichment filters due to the analysis of a single split islet preparation (cytokine-treated or not), without mock immunopurification. Aa sequences are listed according to the number of peptides identified for each source protein. HLA-I restrictions were assigned based on the predicted affinity and stability (NetMHCstabpan). The last column displays the log<sub>2</sub> median FC in peptide content for the IFN- $\gamma$ /TNF- $\alpha$ /IL-1 $\beta$  vs. basal condition (color codes as in Table S1). Source proteins and/or peptides previously identified or not in ECN90  $\beta$  cells are in blue and red, respectively, with peptide length variants marked with an asterisk. The 3 HLA-A2-restricted peptides retained for CD8<sup>+</sup> T-cell studies are highlighted in yellow: a SCG5<sub>186-195</sub> shorter variant with a higher affinity than the previously identified SCG5<sub>186-196</sub> peptide, a newly identified CHGB<sub>440-448</sub> peptide and an IAPP<sub>15-17</sub>/IAPP<sub>5-10</sub> or PTPRN<sub>596-598</sub>/IAPP<sub>5-10</sub> peptide splice aa sequence (VAL/KLQVFL) previously identified in ECN90  $\beta$  cells, which was finally assigned an HLA-A2 restriction based on the HLA-I haplotype of the islet preparation (HLA-A\*02:01/25:01, -B\*39:01/51:01, -C\*12:03/14:02, i.e. sharing only HLA-A2 with ECN90  $\beta$  cells). NA, not available.

Study phase	Group	Case ID	Age (yrs)	Gender (M/F)	T1D duration (wks)	GADA	IA-2A	ZnT8A	Therapy
Screening	Healthy (n=14)	H004N	44	M	NA	NA	NA	NA	NA
		H005N	36	F	NA	NA	NA	NA	NA
		H017N	35	F	NA	NA	NA	NA	NA
		H079O	36	F	NA	NA	NA	NA	NA
		H087N	34	M	NA	NA	NA	NA	NA
		H106S	47	F	NA	NA	NA	NA	NA
		H297S	28	M	NA	NA	NA	NA	NA
		H312C	36	M	NA	NA	NA	NA	NA
		H314C	26	M	NA	NA	NA	NA	NA
		H315C	43	F	NA	NA	NA	NA	NA
		H316C	27	F	NA	NA	NA	NA	NA
		H354C	26	F	NA	NA	NA	NA	NA
		H356C	28	M	NA	NA	NA	NA	NA
		H372C	24	F	NA	NA	NA	NA	NA
			34.5 (24-47)	43% M 57% F					
Validation	T1D (n=10)	D216P	27	M	10.9	+	-	-	Insulin
		D217Db	34	M	19.0	+	NA	NA	Insulin
		L264D	28	F	32.0	+	+	+	Insulin
		D267T	25	F	1.0	+	NA	NA	Insulin
		D287T	30	M	4.1	+	NA	NA	Insulin
		D314D	44	F	0.6	+	+	+	Insulin
		D324D	28	F	11.3	+	+	NA	Insulin
		D325D	19	M	0.3	-	-	+	Insulin
		D327V	34	F	0.7	+	-	NA	Insulin
		D339V	29	M	0.4	+	+	NA	Insulin
				28.5 (19-44)	50% M 50% F	2.6 (0.3-32.0)			
	Healthy (n=10)	H015T	30	M	NA	NA	NA	NA	NA
		H170S	34	F	NA	NA	NA	NA	NA
		H172O	33	F	NA	NA	NA	NA	NA
		H192C	25	F	NA	NA	NA	NA	NA
		H193C	45	F	NA	NA	NA	NA	NA
		H227C	26	M	NA	NA	NA	NA	NA
		H230C	29	F	NA	NA	NA	NA	NA
		H245C	22	M	NA	NA	NA	NA	NA
		H314C	26	M	NA	NA	NA	NA	NA
		H354C	26	F	NA	NA	NA	NA	NA
			27.5 (22-45)	40% M 60% F					

**Table S4. Related to Fig. 4-5. Characteristics of HLA-A2<sup>+</sup> study subjects for ex-vivo MMr studies on PBMCs.** The healthy donors analyzed in Fig. 4 (screening phase) and the T1D and age/sex-matched healthy donors analyzed in Fig. 5 (validation phase) are listed. The distribution of age, gender and T1D duration is shown at the bottom of each list (median and range for numerical variables). GADA, IA-2A, ZnT8A, anti-GAD, -IA-2 and -ZnT8 aAbs, respectively; NA, not available or not applicable.



	nPOD case	Sex	Age (yrs)	T1D T2D (yrs)	Positive aAbs	C-peptide (ng/ml)	Pancreas MMr <sup>+</sup>					IAPP	PLN MMr <sup>+</sup>				
							IAPP	ISL1	UCN3	ZnT8	MelanA		IAPP	ISL1	UCN3	ZnT8	MelanA
T1D (n=9)	6070	F	23	7	IA-2/mIAA	<0.05			39	74	0				32	0	
	6161	F	19	7	IA-2/mIAA	<0.05	110	59		124	0	0	0		1176	0	
	6211	F	24	4	GAD/IA-2/ZnT8/mIAA	<0.05	29	32		30	0	103	45		60	54	
	6212	M	20	5	mIAA	<0.05	19	29		0		0	0		0		
	6237	F	18	12	GAD/mIAA	<0.05			8	267	0			0	0		
	6242	M	39	19	IA-2/mIAA	<0.05	33	9		66	0	0	0		101	0	
	6243	M	13	5	mIAA	0.42	47	17		0		72	34		209	0	
	6258	F	39	37	mIAA	<0.05			19	118	0			0	299	0	
	6325	F	20	6	GAD/IA-2	0.14			28	28	0			35	0	0	
aAb+ (n=9)	6080	F	69	NA	GAD/mIAA	1.84	38	39		55	25	43	41		50	61	
	6101	M	65	NA	GAD	26.18	36	30		0		0	0		0		
	6123	F	23	NA	GAD	2.01	22	48		0		0	0		0		
	6151	M	30	NA	GAD	5.49			9	28	0						
	6154	F	49	NA	GAD	<0.05			21	64	0						
	6171	F	4	NA	GAD	8.95	13	9		37	0	0	0		0		
	6347	M	9	NA	mIAA	3.26	15	7		33	0	66	60		60	191	
	6388	F	25	NA	GAD/mIAA	1.38			0	34	0			0	35	0	
	6397	F	21	NA	GAD	12.8			6	42	0			0	189	0	
No diabetes (n=12)	6103	M	2	NA	—	0.98			0	55	0			0	0		
	6174	M	21	NA	—	3.00	0	0				28	0				
	6179	F	20	NA	—	2.74			0	96	0			67	150	0	
	6182	M	3	NA	—	2.28			4	23	0			89	163	65	
	6227	F	17	NA	—	2.75			18	3	0			0	0		
	6234	F	20	NA	—	6.89			0	6	0			0	0		
	6254	M	38	NA	—	6.43	0	0		0		0			0		
	6271	M	17	NA	—	11.47	0	5		0		0	0		0	0	
	6287	F	57	NA	—	4.75	7	8		4	0	0	0		0		
	6289	M	19	NA	—	8.05	0	6		0		55	0		0		
	6357	M	5	NA	—	8.82	9	29		0		32	0		0		
	6366	F	21	NA	—	0.41	14	24		0		55	0		0		
T2D (n=4)	6028	M	33	17	—	22.40		25		0			0		0		
	6059	F	19	0.3	—	10.68	12			0		0			107	0	
	6273	F	45	2	—	3.17	13	7				0	0				
	6275	M	48	2	—	3.46	0			0		133	117		0		

**Table S5. Related to Fig. 6. nPOD cases analyzed by *in-situ* tissue MMr staining.** The clinical characteristics of each case are reported along with the counts ( $\times 10^{-3}$ ) of MMr<sup>+</sup> cells/mm<sup>2</sup> pancreas and PLN section area for each of the indicated peptides. Positive sections are marked in red. Case #6287 (presenting a circumscribed neuroendocrine tumor in the pancreatic pan-body region; pan-tail region analyzed here) was classified as a non-diabetic control. NA, not applicable; mIAA, micro-insulin aAbs.

<b>Lasers and filters</b>	<b>Photomultiplier tubes (PMTs)</b>					
<b>488 nm blue laser</b>	C	B	A			
Long pass (LP) filter	\	502	655			
Band pass (BP) filter	488/10	530/30	695/40			
Fluorochrome	SSC	FITC				
<b>561 nm yellow-green laser</b>	E	D	C	B	A	
Long pass (LP) filter	\	600	635	685	735	
Band pass (BP) filter	582/15	610/20	660/20	710/50	780/60	
Fluorochrome	PE	PE-CF594			PE-Cy7	
<b>633 nm red laser</b>	C	B	A			
Long pass (LP) filter	\	710	750			
Band pass (BP) filter	660/20	730/45	780/60			
Fluorochrome	APC		APC-H7			
<b>405 nm violet laser</b>	F	E	D	C	B	A
Long pass (LP) filter	\	502	595	630	675	750
Band pass (BP) filter	450/50	525/50	605/20	655/8	710/50	780/60
Fluorochrome	BV421	L/D Aqua		BV650	BV711	BV786

**Table S6. Related to STAR Methods. Configuration of the flow cytometer used for HLA-A2 MMr assays. L/D, Live/Dead.**